中国科学: 地球科学 2020 年 第 50 卷 第 12 期: 1748 ~ 1769
SCIENTIA SINICA Terrae earthcn.scichina.com
《中国科学》杂志社 SCIENCE CHINA PRESS

综 述

深俯冲地壳的折返: 研究现状与展望

刘贻灿*, 张成伟

中国科学院壳幔物质与环境重点实验室, 中国科学技术大学地球和空间科学学院, 合肥 230026
* 通讯作者, E-mail: liuyc@ustc.edu.cn

收稿日期: 2019-12-27; 收修改稿日期: 2020-05-30; 接受日期: 2020-06-03; 网络版发表日期: 2020-07-24
国家重点基础研究发展计划项目(编号: 2015CB856104)和国家自然科学基金项目(批准号: 41773020)资助

摘要 表壳岩中柯石英和金刚石等标志性超高压变质矿物及相关证据的发现表明, 地壳岩石可以俯冲到地幔深度, 经历超高压变质作用并折返至地表. 然而, 深俯冲地壳岩石的折返一直是地球动力学研究领域的热门话题, 并长期存在争议. 前人对深俯冲地壳岩石的折返过程与机制进行了大量的自然观测、类比实验和数值模拟, 取得了一些重要成果. 文章系统总结了近年来关于俯冲带类型、深俯冲地壳的折返过程和机制及其影响因素等方面的研究进展和存在的问题. 在此基础之上, 提出了有关深俯冲地壳折返方面的三个未来研究方向: (1) 折返地壳内部的地质过程; (2) 折返地壳与地表过程的相互作用; (3) 折返地壳与地幔相互作用.

关键词 俯冲带, 高压变质, 超高压变质, 地壳折返, 地壳拆离, 变质*P-T-t*轨迹

1 引言

表壳岩中柯石英和金刚石等标志性超高压变质矿物的发现表明, 地壳岩石可以俯冲到大于80km的地幔深度, 经历超高压变质作用并折返至地表(Chopin, 1984; Smith, 1984; Sobolev和Shatsky, 1990; Xu等, 1992). 目前, 全球已陆续发现三十余条超高压变质带(Liou等, 2014; Yan和Zhang, 2019). 然而, 俯冲地壳如何折返至地表, 尤其是出露面积大于25000km^{2}的挪威西部片麻岩省、中国大别-苏鲁和柴北缘高压-超高压变质地体(Kylander-Clark等, 2012; 郑永飞等, 2013)等是如何折返至地表的, 一直存在争议(Liu等, 2007b; 刘贻灿和李曙光, 2008; Hacker等, 2013; Ducea, 2016, 以及所引文献), 且是地球动力学研究领域的热点和前沿问题(刘贻灿等, 2015). 这些超高压变质带为我们研究俯冲带及其深部地质过程提供了重要的天然实验室, 而且, 深入研究地壳的俯冲与折返过程, 对发展板块构造理论具有重大科学意义. 此外, 俯冲地壳在折返期间的部分熔融常常形成同折返岩浆岩(Zhao等, 2017), 并引起地壳成分的改造和大陆地壳的生长(Niu等, 2013). 同时, 俯冲地壳的折返过程(或机制)还会影响到物质再循环和地壳成分的分异, 以及地幔不均一性和有关成矿作用等(如Kessel等, 2005; Zheng, 2012; Chen等, 2019).

然而, 研究俯冲地壳折返机制常常受到一定条件的限制, 主要表现在: (1) 俯冲地壳折返持续时间以百万年为单位, 无法直接进行动态观测. 为了解俯冲和折返过程, 需要一系列的自然观测反演、类比实验和数值正演模拟(Chemenda等, 1995; Ernst等, 1997; Xu等, 2006; Liu等, 2007b; 刘贻灿和李曙光, 2008;

中文引用格式: 刘贻灿, 张成伟. 2020. 深俯冲地壳的折返: 研究现状与展望. 中国科学: 地球科学, 50(12): 1748–1769, doi: 10.1360/SSTe-2019-0307
英文引用格式: Liu Y, Zhang C. 2020. Exhumation of deeply subducted crust: Review and outlook. Science China Earth Sciences, 63(12): 1904–1924, https://doi.org/10.1007/s11430-019-9639-9

© 2020 《中国科学》杂志社

Warren, 2013; Burov等, 2014a), 数值和类比模拟结果均需要经过自然观测验证; (2) 仅部分高压-超高压变质岩出露地表, 且后期受到不同程度的退变质作用、岩浆作用和构造作用等的叠加与改造, 甚至可能经历了两个造山循环(Herwartz等, 2011; Rubatto等, 2011; Ren等, 2019); (3) 变质*P-T-t*轨迹条件恢复具有一定的局限性(Lü和Bucher, 2018; 吴春明, 2018; Cutts等, 2019), 这为俯冲地壳折返过程的变质*P-T-t*演化轨迹的重建造成了一定困难. 目前, 西太平洋伊豆-小笠原-马里亚纳(Izu-Bonin-Mariana, IBM)俯冲带是全球唯一正在借助蛇纹岩泥火山折返的大洋型俯冲带(Tamblyn等, 2019), 巴布亚新几内亚(Papua New Guinea, PNG)出露世界上最年轻的柯石英榴辉岩, 峰期变质年龄仅(7.1±0.7)~(4.61±0.18)Ma(Gordon等, 2012). 这些年轻的造山带为我们研究俯冲地壳折返提供了宝贵的资料.

二十多年来, 前人对深俯冲地壳折返机制进行了大量的探讨(Liu等, 2007b; Guillot等, 2009; 杨经绥等, 2009; Hacker和Gerya, 2013; Warren, 2013; 郑永飞等, 2013; Burov等, 2014a; 张立飞和王杨, 2020), 滋生了新的科学发现和问题. 本文总结了已报道的高压-超高压变质岩的折返过程和折返机制, 并探讨其未来的发展方向. 首先, 我们简单介绍了俯冲带的类型; 其次, 从自然观察、类比实验和数值模拟等方面, 回顾了深俯冲地壳岩片从俯冲到地幔深度→折返至地表的复杂地质过程, 简要讨论了折返驱动力和折返构造背景; 最后提出了存在的相关科学问题和未来的研究方向.

2 俯冲带类型

根据俯冲岩石圈性质的不同, 俯冲带可以分为大洋俯冲带和大陆俯冲带(Ernst, 2005; Zheng和Chen, 2016). 根据地温梯度的不同, 俯冲带又可以分为暖俯冲和冷俯冲(Peacock和Wang, 1999; van Keken等, 2011; Abers等, 2013; Angiboust等, 2017; Fossen等, 2017). 它们在原岩建造和岩石组合以及变质*P-T-t*轨迹与熔流体活动等方面存在显著差异, 进而导致俯冲板片折返过程具有不同的表现. 而且, 不同时代和不同热状态的板片在俯冲期间具有不同的变质*P-T*轨迹(Wada和Wang, 2009; 郑永飞等, 2016).

2.1 大洋和大陆俯冲带

大洋俯冲带以大洋岩石圈俯冲为特征. 大洋俯冲带发育典型的海沟、火山弧和双变质带, 环太平洋地区是典型代表(Ernst, 2005). 相对年轻、热的俯冲洋壳能够发生部分熔融(Defant和Drummond, 1990; Niu等, 2013; Song等, 2014a). 洋壳榴辉岩的折返*P-T-t*轨迹可以归纳为三类(Agard等, 2009; 陈意和叶凯, 2013): (1) 近等温降压型(主要的), 一般代表快速的折返过程; (2) 降温降压型, 代表了缓慢抬升的过程; (3) 降压升温型(极少数). 相平衡模拟和密度计算表明, 前两种洋壳榴辉岩折返过程中密度降低促进折返, 而第三种从最高压力峰折返到最高温度峰过程中, 密度增加而折返速率降低(Wang Y等, 2019).

大陆俯冲带以大陆岩石圈俯冲为特征, 陆壳平均密度比洋壳岩石低, 相对贫水且黏度高, 以出露超高压变质岩、缺乏同俯冲岩浆作用为特征(Ernst, 2005; Zheng和Chen, 2016). 俯冲陆壳在折返过程中, 不同类型变质岩可能发生低程度的部分熔融(Hermann和Green, 2001; Auzanneau等, 2006; Labrousse等, 2011; Zheng等, 2011; Zhao等, 2017). 陆壳折返速率比洋壳快(Agard等, 2009). 近期大量统计数据表明, 二者峰期变质条件近似(Brown和Johnson, 2019). 然而, 陆壳俯冲-折返的变质*P-T-t*轨迹呈顺时针, 而且, 折返早期表现为近等温减压或降温减压过程, 到达中-下地壳后趋于等压降温(Kylander-Clark等, 2012; Hermann和Rubatto, 2014; Liu等, 2015).

2.2 冷俯冲和暖俯冲

俯冲带热结构显著影响板片流变学性质, 进而影响板片拆离折返(Gerya等, 2004; 郑永飞等, 2016). 一方面, 俯冲带热结构随地球演化不断改变(Brown, 2006; Hawkesworth等, 2016; Zheng和Zhao, 2020). 地幔温度从约30亿年前最高约1500~1600℃降低到目前约1300~1350℃(Herzberg等, 2010; Hawkesworth等, 2016; Weller等, 2019). 地幔温度低, 与固相线交点的深度低, 地幔部分熔融深度则越浅; 反之, 地幔温度高, 部分熔融深度越深. 地幔温度影响洋壳的厚度、成分和密度演化和浮力(White等, 1992; Langmuir等, 1992; Weller等, 2019). 另一方面, 不同大洋俯冲带热结构也存在差异(Peacock和Wang, 1999), 而大陆俯冲带地温

梯度普遍较低(<10℃ km^{-1})(Liou等, 2009; Zheng和Chen, 2016). 俯冲带地温梯度高, 板片强度低, 导致板片断离频繁, 不利于板片深俯冲(Sizova等, 2010; Moyen和van Hunen, 2012).

根据地热梯度差异, 大洋俯冲带可以分为冷俯冲和暖俯冲, 二者在变质反应、弧岩浆作用、地震活动等方面存在显著差异(Peacock和Wang, 1999; van Keken等, 2011; Abers等, 2013; Zheng和Chen, 2016). 俯冲带热结构主要受板片年龄和汇聚速率控制(McKenzie, 1969; Zheng, 2019), 年龄越小, 汇聚速率越慢, 而板片表面温度越高, 反之则越低. 如果暖俯冲洋壳在弧前地幔浅部(<60km)显著脱水, 在弧下深度(80~160km)则难以析出大量流体, 结果会相对缺乏岛弧岩浆作用, 而洋壳在冷俯冲带能够将流体带到弧下地幔, 并形成大量岛弧火山岩(郑永飞等, 2016). 折返的大洋榴辉岩普遍来自于冷俯冲带(Chen等, 2013), 记录的地温梯度一般介于8~10℃ km^{-1}, 最高不超过15℃ km^{-1}(Agard等, 2009), 部分也存在超冷俯冲带, 如西南天山(Zhang等, 2018). Penniston-Dorland等(2015)发现, 高压蓝片岩和榴辉岩记录的温度比俯冲带热结构模型高100~300℃, 认为当前俯冲带热结构模型并不准确, 可能低估了剪切热的作用. 而van Keken等(2018)、Hernández-Uribe和Palin(2019)指出, 热模型中加入剪切热与不添加相比, 升温低于50℃. 他们认为, 榴辉岩和蓝片岩更倾向于在暖俯冲带折返, 因为暖俯冲脱水流体有利于俯冲板片和地幔楔界面力学解耦.

自然观测和实验模拟表明, 陆壳流变性和碰撞造山带演化也受热结构控制(Burov和Yamato, 2008; van Hunen和Allen, 2011; Moyen和van Hunen, 2012; Sizova等, 2014; Fossen等, 2017). Sizova等(2014)通过数值模拟发现, 如果上部地幔温度比当前高80~100℃, 陆壳在浅部就发生板片断离, 因此将缺乏大陆深俯冲和没有超高压变质岩的形成. Burov和Yamato(2008)发现, 大陆俯冲随莫霍面温度(T_{Moho})升高而失稳, 只有当刚性的岩石圈莫霍面温度低于550℃且汇聚速度较快(5~15cm a^{-1}), 才可能发生陆壳深俯冲及高压-超高压变质岩折返. 因此陆壳深俯冲均发生在冷俯冲带, 部分地温梯度甚至≤5℃ km^{-1}(Liou等, 2009). Fossen等(2017)通过对比冷和热的碰撞造山带, 进一步证实了上述结论.

3 俯冲地壳的折返过程

地壳俯冲和折返期间形成了不同等级的变质岩(Liu Y C等, 2007b, 2017; Xu等, 2012; 郑永飞等, 2013; Li等, 2020b). 其中, 部分岩石从俯冲板片拆离并折返出露地表(图1a、1b、1d)(Chopin, 1984; Smith, 1984; Sobolev和Shatsky, 1990; Xu等, 1992)(图1), 并伴随地幔楔折返(Guillot等, 2001; Deschamps等, 2013; Solarino等, 2018), 部分底垫于仰冲盘或上盘(Warren等, 2008b; Nábělek等, 2009; Hacker等, 2011; Schliffke等, 2019)(图1c), 而另一部分则参与地幔再循环. 根据自然样品观测、实验和数值模拟结果, 前人提出了不同的俯冲地壳折返模型(Platt, 1993; Ernst等, 1997; Her-

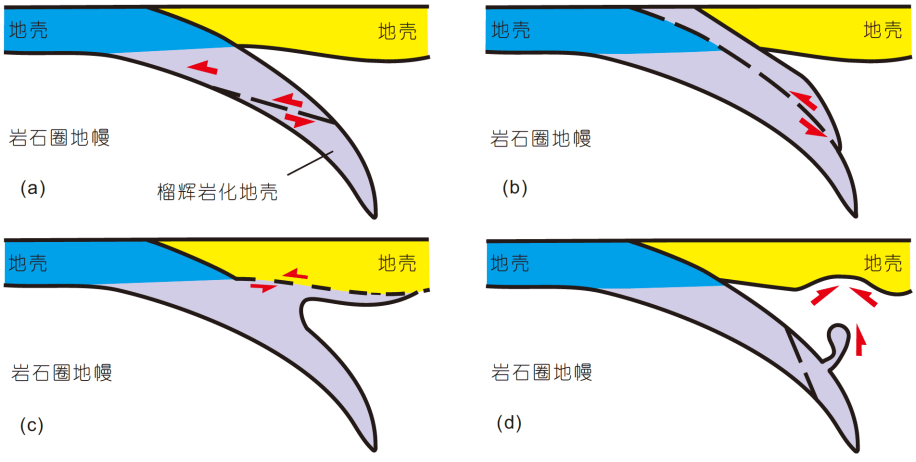


图 1　俯冲地壳岩石的去向示意图

部分俯冲进入地幔深部, 部分呈整体折返(a)、沿俯冲隧道折返(b)、底垫到上盘(c)以及底辟折返(d)

mann等, 2000; Xu等, 2006; Liu等, 2007b; Yin等, 2007; 刘贻灿和李曙光, 2008; Agard等, 2009, 2018; 杨经绥等, 2009; Labrousse等, 2011; Li等, 2011; Little等, 2011; Malusà等, 2011, 2015; Kylander-Clark等, 2012; Chen等, 2013; Hacker和Gerya, 2013; Warren, 2013; 郑永飞等, 2013; Burov等, 2014a; Erdman和Lee, 2014; Liao等, 2018; Wang Y等, 2019; 张立飞和王杨, 2020), 并促进了一系列新的科学发现.

3.1　深俯冲地壳的拆离解耦

深俯冲地壳的拆离解耦主要涉及三种情况: 板片与地幔楔解耦(Faccenda等, 2009; 郑永飞等, 2016; Agard等, 2018)、俯冲地壳内部拆离(刘贻灿和李曙光, 2008; Carry等, 2009; 郑永飞等, 2013)和板片断离(slab breakoff)(Davies和von Blanckenburg, 1995). 板块界面耦合和解耦取决于俯冲带地幔楔流变性、黏度差异、起始结构(如不均一的岩石圈、拆离带的存在和水化程度等)以及汇聚速率、运动学等边界条件(Agard等, 2018). 而且, 高的汇聚速率和熔/流体渗透率有利于板块间的解耦(Faccenda等, 2009). 基于全球俯冲洋壳岩石单位的重要观测和系统总结, Agard等(2018)提出板块界面耦合和解耦之间的过渡区是俯冲洋壳拆离折返最有利的位置. 俯冲洋壳-地幔楔界面70~80km深度发生力学耦合-解耦转变(Abers等, 2006; Wada和Wang, 2009; Agard等, 2018). 目前俯冲陆壳-地幔楔-耦合-解耦转变的深度尚缺乏限定. 由于陆壳浮力作用引起俯冲速率降低, 脱水作用较弱. 与大洋型俯冲相比, 推测俯冲陆壳与地幔界面耦合-解耦转变深度应该小于70km. 岩石学表明, 部分陆壳俯冲深度>200km(Ye等, 2000; Liu L等, 2007). 因此, 深俯冲陆壳与上覆地幔楔在浅部(<70km)经历了耦合-解耦的空间转变.

当承受的应力高于屈服强度时, 俯冲地壳内部拆离, 拆离的地壳规模主要依次受俯冲角度、地壳流变性、地幔热流值和俯冲速率等因素控制(Carry等, 2009). 二维数值模拟表明, 在相同俯冲深度, 俯冲角度越大, 地壳流变性越弱, 地幔热流值越高, 俯冲速度越快, 越有利于俯冲地壳拆离(Carry等, 2009). 前人提出了引起深俯冲板片内部拆离的多种弱化机制, 包括应变弱化、水化、部分熔融、矿物粒径减小和面理发育等(Warren, 2013). 然而, 高应变薄弱带的形成时间、确切位置和主导机制都很难确定(李忠海, 2014), 需要开展更多的限定和定量化方面的研究.

此外, 在大陆碰撞期间, 当大陆岩石圈与大洋岩石圈发生断离时, 陆壳俯冲动力消失, 深俯冲地壳将发生折返(Davies和von Blanckenburg, 1995). 区域地质和地球物理资料表明, 俯冲板片局部是不连续的, 产生的机制包括垂向板片撕裂(slab tear)(图2b)(近平行于板片汇聚方向)(Xiao等, 2007; Chen等, 2015; Zhang等, 2019)和水平方向(沿俯冲带展布方向)的板片断离(图2c~2e)(Davies和von Blanckenburg, 1995; Rosenbaum等, 2008). 板块初始断离方式可能从一侧(图2c)(Wortel和Spakman, 2000)、两侧(图2d)(Gerya等, 2004)或从中部开始(图2e)(van Hunen和Allen, 2011; Pusok等, 2018), 形成对称或不对称的断离构造(breakoff structure)(Wortel和Spakman, 2000; Gerya等, 2004), 具体取决于俯冲板片的热力学结构. 前人对板片断离进行了不同边界条件的平面和三维数值模拟(Dabies和von Blanckenburg, 1995; Gerya等, 2004; Duretz等, 2011; van Hunen和Allen, 2011; Burov等, 2014b)以及类比实验(Boutelier和Cruden, 2017; Fernández-García等, 2019), 研究结果表明, 板片断离时间、深度和形式受板块年龄、厚度、汇聚速率、热结构、应变速率和流变性等影响. 板片断离常出现在40~400km深度(Duretz等, 2011). 俯冲速率越快, 俯冲板片越古老, 岩石圈强度越大, 断离起始的深度越大(Baumann等, 2010; Burov等, 2014a). 板片断离速率约在30~40到~1000mm a^{-1}之

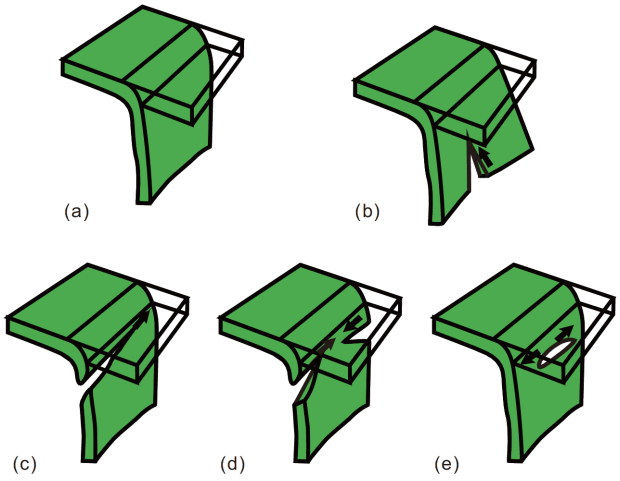


图 2　俯冲板片的撕裂和断离示意图

(a) 初始俯冲板片; (b) 板片撕裂; (c)~(e) 分别从一侧、两侧和内部发生板片断离, 修改自Gerya等(2004)、Rosenbaum等(2008)、van Hunen和Allen(2011)、Boutelier和Cruden(2017)

间变化(Boutelier和Cruden, 2017). 板片拆离起止时间可小于1个百万年, 且与拆离的起始深度无关(Duretz等, 2012; Bercovici等, 2015). 矿物的相变有助于加速俯冲板片断离, 并引起断离深度增加(Baumann等, 2010). Fernández-García等(2019)开展了一系列三维洋-陆转变带几何形态与板片断离类比模型试验, 发现被动边缘与海沟之间的几何形态决定了俯冲板片断离的深度和起始位置: (1) 被动边缘与海沟平衡时, 俯冲板片从中部开始断离; (2) 被动边部先到达俯冲带时, 该处先发生板片断离, 之后向中部扩展, 且板片断离深度更深. Warren等(2008a)通过数值模拟研究了板片断离对地壳折返的影响, 认为板片断离并不是超高压变质岩折返的必要条件. 板片断离可能引起软流圈上涌, 造成俯冲地壳加热, 促进超高压岩石的部分熔融、拆离解耦和折返(Warren, 2013).

3.2 深俯冲地壳的折返路径

深俯冲地壳的折返方式, 可以归纳为两种类型(Wang和Cong, 1999). 第一种, 超高压变质岩穿过上覆板片, 包括俯冲隧道折返(Liu M Q等, 2017)和底辟折返(Hall和Kincaid, 2001; Yin等, 2007; Little等, 2011)两种方式; 第二种, 上覆岩石经构造减薄(如伸展减薄、山根垮塌)或(和)剥蚀作用被移除, 引起俯冲地壳岩石出露地表. 其中第一种占主要地位, 而第二种发挥次要作用. 折返的驱动力见下文, 下面概述俯冲隧道折返(图1b)和底辟折返(图1d)两种模型.

俯冲隧道是指汇聚板块边缘俯冲板片与上覆板片之间的剪切带(Shreve和Cloos, 1986; Cloos和Shreve, 1988; Gerya等, 2002; 郑永飞等, 2013). 俯冲隧道折返模型已经被数值模拟(Gerya等, 2002)所证实. 厚的上覆大陆岩石圈和年轻的大洋板片低角度俯冲都有助于相对冷的俯冲隧道的形成并会引起高压-超高压岩石沿俯冲隧道折返(Liu M Q等, 2017). Butler等(2011)根据数值模拟认为, 沿俯冲带折返, 超高压变质岩可能出露在下盘, 也可能由于上盘强度相对较弱而折返、挤入至上盘(图3). 上述模型是根据两盘深部物理边界得出的结论. 但是, 尽管浅部缝合线与深部两盘边界不一致, 根据浅部缝合线位置, 超高压变质岩仍出露于下盘.

当超高压变质岩密度和黏度足够低, 可能发生底辟折返(图1d)(Platt, 1993). 俯冲洋壳上覆地幔楔可能出现底辟流(diapiric flow), 形成低密度和低黏度的管状通道, 进而快速上升至地壳浅部(Hall和Kincaid, 2001). 数值模拟结果表明, 俯冲带部分沉积物能够从俯冲板片拆离、形成近水平的沉积柱状体并进入浅部弧后地幔(Currie等, 2007). 此外, 岛弧岩浆具有大洋沉积物的地球化学特征. 根据热模型, Behn等(2011)发现, 在2.5~5GPa时大洋沉积物以固态形式拆离并底辟进入了地幔楔. 数值模拟也表明俯冲带会形成冷地幔柱(cold plume)底辟进入地幔楔(Castro和Gerya, 2008). 上覆板片中的伸展断层有利于深俯冲地壳岩石沿断裂底辟上升至地壳浅部(Tamblyn等, 2019). 薄的上覆大陆岩石圈及高角度俯冲的老的洋壳有助于形成热的俯冲隧道并引起高压-超高压岩石发生底辟折返(Liu M Q等, 2017). 一些研究者认为, 柴北缘、巴布亚新几内亚、喜马拉雅Tso Morari超高压变质岩通过底辟折返(Yin等, 2007; Little等, 2011; Chatterjee和Jagoutz, 2015), 但仍存在争议(Petersen和Buck, 2015; Liu M Q等, 2017; O'Brien, 2019).

3.3 整体折返与多岩片差异折返

关于超高压变质岩的折返模式, 大多数模型都假定整个俯冲陆壳与下伏岩石圈地幔发生拆离解耦并整体折返, 如陆内逆冲及伴随侵蚀模式(Chemenda等,

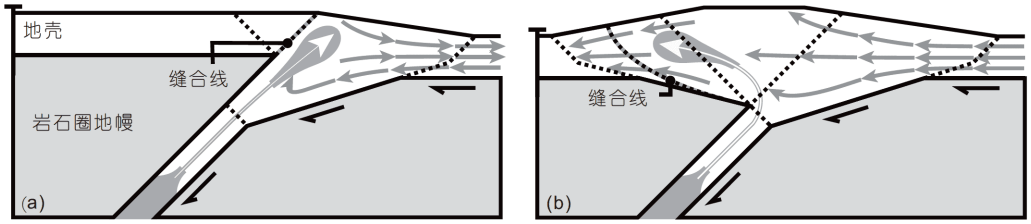


图 3 沿俯冲带折返时, 超高压变质岩可能出现在下盘(a)或上盘(b)

据Butler等(2011)

1996)、挤出-伸展模式(Maruyama等, 1994; Faure等, 1999)、浮力驱动模式(Ernst等, 1997)、角流及浮力联合模式(Wang和Cong, 1999)、平行于造山带的挤出及伴随减薄模式等(Hacker等, 2000; Ratschbacher等, 2000)以及挤出(eduction)折返模型(图1a)(Andersen等, 1991). Burov等(2001)对大陆俯冲带进行热力学数值模拟, 证明俯冲板片在不同深度发生多阶段拆离折返, 且具有不同折返机制(图4), 因此, 世界上不同的深俯冲地壳岩石常常具有不同的变质*P-T-t*轨迹(Liu等, 2011, 2015; Yamato和Brun, 2017). 此外, 系统的同位素年代学、岩石学、地球化学和构造地质学等方面研究均表明, 俯冲碰撞造山带内部不同的岩石构造单元可能来自不同的地壳层次, 记录了不同的峰期变质压力-温度-时间, 且以断裂带为边界, 指示俯冲陆壳内部经历多层次拆离解耦和多岩片差异折返, 如大别-苏鲁碰撞造山带(图5)(李曙光等, 2005; 刘贻灿和李曙光, 2005, 2008; Xu等, 2006; Liu等, 2007b, 2017; 郑永飞等, 2013; Li等, 2020b).

张立飞等(2008)以西南天山和柴北缘为例, 介绍了大洋型超高压变质带的地质特征, 指出洋壳深俯冲超高压变质岩的原岩组合保存相对完整、变质程度没有明显区别, 属于整体俯冲和抬升过程, 与大陆深俯冲拆离解耦截然不同. 西南天山哈布腾苏-科布尔(Habutengsu-Kebuerte)流域柯石英的发现和峰期*P-T-t*条件重建结果表明, 不同类型的变质岩共同经历了超高压变质作用和整体折返(2.8~3.5GPa/520~580℃)(Lü等, 2012; Zhang等, 2013, 2018; Lü和Bucher, 2018), 而不是构造混杂(Meyer等, 2016). 西南天山除了超高压变质带, 也存在高压变质带(Zhang等, 2018), 因此该区俯冲洋壳的折返可能也经历了多层次拆离折返. Li等(2016)发现西南天山部分榴辉岩中蓝闪石和冻蓝闪石交替生长, 暗示其经历了复杂的多期俯冲和折返过程.

3.4　多阶段折返

岩石学研究表明, 欧洲矿石山(Massonne, 2001, 2003)、大别山(Xu等, 2000, 2003; Liu等, 2007a, 2011, 2015; Deng等, 2019)、南阿尔金(Liu等, 2012)、柴北缘(Song等, 2014a, 2014b)和西南天山(Zhang等, 2018)等地超高压变质岩在折返期间经历了麻粒岩相变质叠加和角闪岩相退变质作用等. 类似地, 多种同位素年代学结果也表明, 俯冲地壳经历了多阶段折返过程(Li等, 2000; Liu Y C等, 2007b, 2011; Gordon等, 2012; Liu L P等, 2017; Cutts等, 2019). 此外, Duchêne等(1997)综合前人研究发现, 起初地壳折返速率(>1mm a^{-1})很快, 但仅持续几个百万年至数十百万年, 而和第一阶段相比, 最终抬升速率至少下降了一个数量级. 因此, 深俯冲地壳经历了多阶段折返.

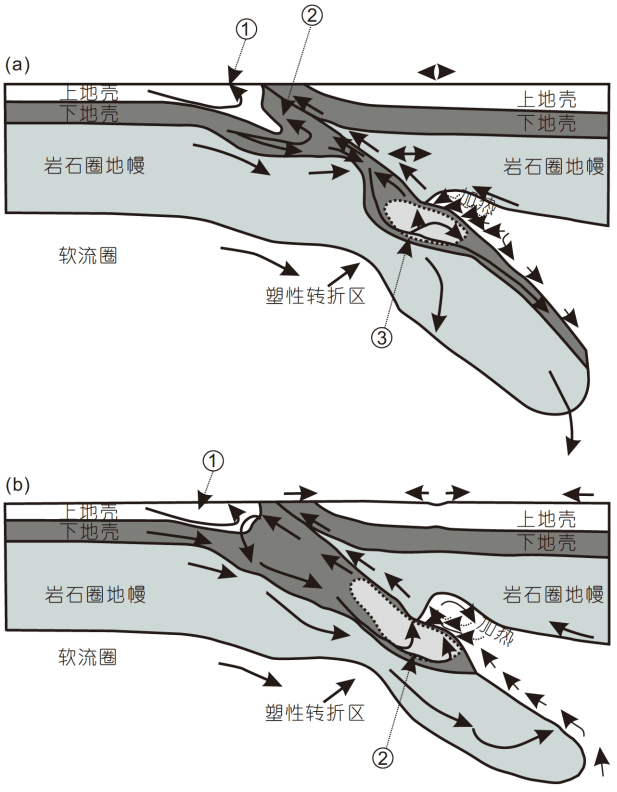


图 4　俯冲地壳岩石折返的两种热力学数值模拟结果

(a) 完全榴辉岩化(低浮力): ①LP-LT角流折返、②HP-HT折返和③UHP-UHT/HP-HT折返; (b) 低榴辉岩化(高浮力): ①LP-LT角流折返和②UHP-UHT/HP-HT折返. 据Burov等(2001)

3.5　部分熔融作用

实验岩石学和数值模拟研究表明, 部分熔融作用是弱化地壳岩石力学强度(Rosenberg, 2001)、降低密度(Gerya等, 2004)的重要因素, 而且, 当熔体体积达到7~20%时能够显著弱化板片(Rosenberg和Handy, 2005)并强烈影响俯冲板片的折返动力学(Labrousse等, 2015). 自然观测表明, 折返陆壳(Hwang等, 2006; Liu等, 2014; Wang等, 2014; Ferrero等, 2015; Labrousse等, 2015; 刘贻灿等, 2015; Zhao等, 2017; Deng等, 2018, 2019; Li等, 2020a)和洋壳(Niu等, 2013; Song等, 2014a)

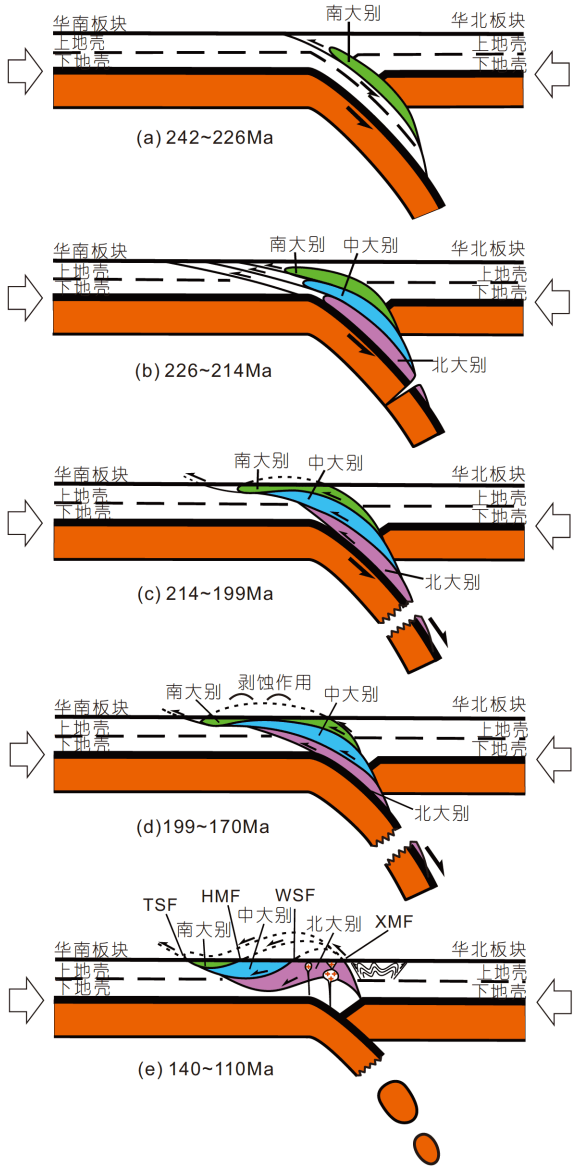


图 5　大别造山带多岩片多阶段差异折返示意图

TSF, 太湖-山龙断裂; HMF, 花凉亭-弥陀断裂; WSF, 五河-水吼断裂; XMF, 晓天-磨子潭断裂. 据Liu等(2011)

会发生不同程度的部分熔融作用. 折返板片部分熔融可能主要是板片减压折返引起的, 同时又能够进一步促进折返, 是导致不同深度俯冲地壳折返的重要因素(Faccenda等, 2008; Deng等, 2018). 数值模拟定量研究了部分熔融在板片折返中的作用(Gerya等, 2008; Faccenda等, 2009; Labrousse等, 2015). Labrousse等(2015)指出, 饱水熔融时板片在碰撞后会快速折返, 而脱水熔融则不会显著改变俯冲-碰撞动力学. 因此, 部分熔融作用被认为是弱化俯冲地壳岩石强度和促进地壳折返的极其重要因素(Warren, 2013). 此外, 有些超高压地体表现为冷的地温梯度、缺乏明显的部分熔融作用(Labrousse等, 2015), 如西阿尔卑斯的Zermatt-Saas带具有大洋属性的超高压岩石(Reinecke, 1998)以及Dora Maira带大陆属性的超高压岩石(Chopin和Schertl, 1999).

3.6　折返速率和规模

从地幔深度折返至中上地壳期间, 不同深俯冲地壳折返速率差异很大(Rubatto和Hermann, 2001; Baldwin等, 2004; Agard等, 2009; Kylander-Clark等, 2012; Hermann和Rubatto, 2014). 大陆俯冲带中, 如大别-苏鲁超高压变质岩从大于120km的地幔深度折返至地壳水平, 折返速率介于3~6mm a^{-1}(Liu等, 2006; Liu等, 2011), 而Kaghan Valley超高压岩石从~100km的地幔深度折返至大陆壳底部(35km的深度)的折返速率达到30~80mm a^{-1}(Parrish等, 2006). 俯冲洋壳折返速率主要在1~5mm a^{-1}, 个别大于5~10mm a^{-1}, 明显低于俯冲陆壳折返速率(Agard等, 2009). 折返速率与流变性(Gerya等, 2002)、出露规模(图6)和造山阶段相关(Kylander-Clark等, 2012). 出露规模小的超高压板片多为新生地壳, 折返速率快, 形成于造山阶段早期; 出露规模大的超高压板片古老, 折返速率较慢, 形成于造山阶段晚期(图6)(Kylander-Clark等, 2012). 郑永飞等(2013)认为, 俯冲隧道内小的地体易于运动, 而大的地体难以运动, 原岩性质和岩石组合控制了超高压变质地体的大小.

当满足牛顿黏性定律时, 折返速率与俯冲板片和周围地幔的密度差、h^2(h代表俯冲隧道宽度)成正比, 俯冲角度正弦值成正比, 与黏度成反比(Erdman和Lee, 2014). 同一类型俯冲带出露的岩性相同, 它们的黏度和密度差也应该类似. 已有研究表明, 如果板片的俯冲角度从60°降低到30°, 折返速率仅降低~0.3cm a^{-1}(Erdman和Lee, 2014). 因此, 板片的俯冲角度对折返速率没有明显影响. 据此推测, 折返速率越低, 暗示俯冲隧道宽度越小. 而且, 冷俯冲带脱水缓慢, 导致浅部上覆地幔楔水化程度低, 俯冲隧道窄. 冷俯冲带板片能将水运送到地幔更深部, 所以冷俯冲带俯冲隧道更长. 也就是说, 冷俯冲隧道更长更窄, 折返速率低但折返规模大. 而热俯冲带浅部脱水程度高, 引起浅部上覆地幔楔弱化程度高, 引起俯冲隧道宽而短, 折返速率高但折返

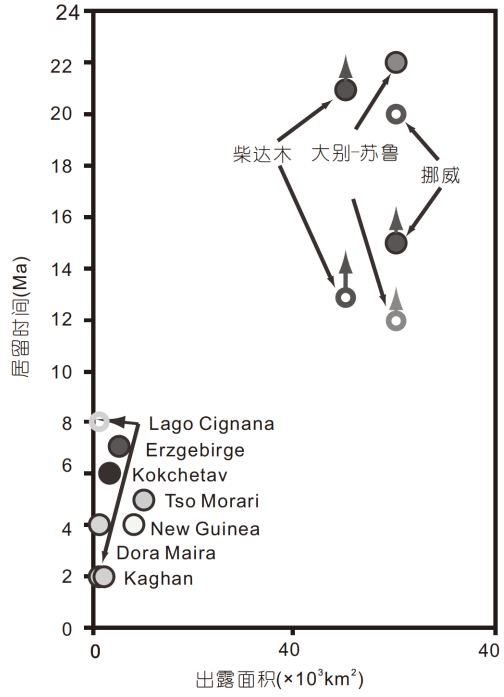


图 6　**板片折返规模与时间的关系**

据Kylander-Clark等(2012)

规模小. 此外, 数值模拟结果表明, 热的俯冲带更有利于镁铁质高压变质岩的折返(van Keken等, 2018); 自然观测则表明大洋榴辉岩均来自于冷俯冲带(Chen等, 2013). 因此, 这一猜想将出露规模和造山带热结构联系在一起、调和了上述矛盾, 同时也与折返速率、出露规模和俯冲带热结构和造山带构造演化等方面的调查结果相吻合.

4　深俯冲地壳折返的驱动力

深俯冲陆壳通常被认为因受正浮力作用而折返(Ernst等, 1997; Agard等, 2010). 近期研究表明, 洋壳折返也可能借助自身浮力折返(Chen等, 2013; Chapman等, 2019; Hernández-Uribe和Palin, 2019; Wang Y等, 2019), 但是, 最大浮力折返深度和折返洋壳岩石类型之间仍存在一些争议. 此外, 外部构造作用力在某些情况下也有利于深俯冲地壳的折返(Platt, 1993; Warren, 2013).

4.1　浮力

众所周知, 大陆俯冲带出露的俯冲陆壳岩石主要是长英质片麻岩, 而榴辉岩体积仅占小部分. 杨建平等(2005)在常温常压下测量了中国大陆科学钻孔100~3000m深度的岩芯样品的密度, 通过深度密度校正发现, 榴辉岩密度随退变质作用程度增加而降低(3.52g cm^{-3}→2.93g cm^{-3}), 而超高压长英质片麻岩密度的变化为3.00g cm^{-3}→2.65g cm^{-3}. 因此, 长英质片麻岩密度小于周围地幔密度(~3.2g cm^{-3}), 长英质片麻岩的俯冲折返过程主要受正浮力控制, 需要高密度镁铁质和超镁铁质岩石圈的拖拽才能深俯冲进入地幔. 此外, Chapman等(2019)利用相平衡模拟获得了镁铁质洋壳和安山质、花岗质陆壳在不同温压条件下的密度变化, 认为俯冲深度<120km时, 安山质陆壳具有正浮力; 花岗质陆壳的最大折返深度在160~260km, 具体取决于水含量. 而且, 当长英质陆壳与高密度镁铁质和超镁铁质岩石圈的比例低于1/3时, 陆壳能够俯冲到85~160km; 然而, 俯冲深度大于160km时, 则要求二者比值高于2/3. 实验岩石学研究表明, 上地壳俯冲深度超过250km(约8~9GPa)时, 便难以依靠自身的浮力折返(Wu等, 2009). Schliffke等(2019)利用数值模拟研究了陆壳与地幔之间密度差($\Delta\rho$)大小对俯冲陆壳折返和相关岩浆作用的影响, 发现$\Delta\rho$>500kg m^{-3}时, 有利于俯冲陆壳沿俯冲隧道折返并伴随小规模的岩浆作用, 而$\Delta\rho$<50kg m^{-3}则有利于俯冲陆壳的底垫和广泛的岩浆活动.

大洋型俯冲带出露的主要是榴辉岩、变沉积岩、蓝片岩和蛇纹岩等. 实验表明大洋榴辉岩密度(~3.6g cm^{-3})大于周围地幔密度(Aoki和Takahashi, 2004), 因此洋壳折返动力普遍认为来自周围低密度岩石浮力, 如增生楔中变沉积岩(Platt, 1986)、低密度陆壳岩石(Burov等, 2014a; Ernst, 2001)或蛇纹岩(Hermann等, 2000). 然而, Chen等(2013)认为俯冲洋壳密度数据来自高温干榴辉岩的实验结果, 但出露地表的洋壳榴辉岩大多数来自冷俯冲带, 因此无法代表冷俯冲大洋榴辉岩密度. 此外, Chen等(2013)通过热力学计算发现, 俯冲洋壳沿冷俯冲*P-t*轨迹演化、地温梯度为~6℃ km^{-1}、俯冲深度小于110~120km(3.3~3.6GPa)时, 密度仍然小于周围地幔; 而洋壳沿热俯冲*P-t*轨迹演化、地温梯度为~10℃ km^{-1}、深度大于60km(>1.8GPa)时, 则榴辉岩变得致密, 密度大于周围地幔. 同时, Chen等(2013)根据洋壳成因榴辉岩的峰期*P-T*条件(图7), 认为其均能够借助自身浮力折返. Agard等

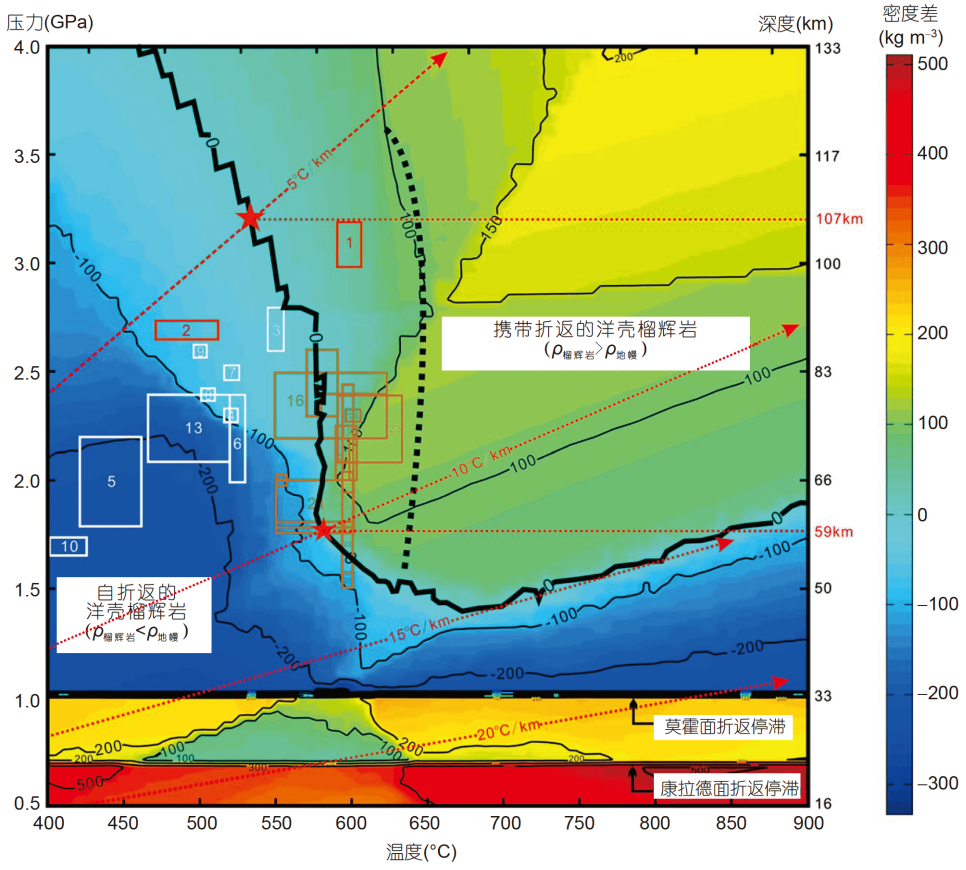


图 7　不同温压条件洋壳与地幔密度差($\Delta\rho$)等值线图

红色长方形代表超高压榴辉岩, 白色长方形代表含硬柱石高压榴辉岩, 棕色长方形代表含绿帘石高压榴辉岩. 黑色实线代表密度差等值线, 黑色粗实线代表$\Delta\rho$=0等值线, 红色虚线代表不同的地温梯度. 黑色粗虚线代表Chen等(2013)计算的密度差曲线$\Delta\rho$=0位置, 具体编号见Chen等(2013). 据Wang Y等(2019)

(2009)计算了折返洋壳的密度与地幔岩密度差, 发现除Zermatt-Saas和部分Voltri、Monviso地区的大洋型榴辉岩外, 其他均具有正浮力, 依靠浮力折返的最大峰期压力约3.5GPa. Xu等(2019)利用金刚石压腔结合同步辐射单晶X射线衍射实验技术, 系统研究了高铁和低铁榴辉岩相石榴石和绿辉石矿物的热状态方程, 根据获得的热弹性参数, 模拟计算发现, 当沿着Eberle等(2002)模型中的地温梯度和正常上地幔条件下, 深度大于110~125km时榴辉岩密度明显高于地幔密度, 与Chen等(2013)模型一致. Wang Y等(2019)指出, 大洋榴辉岩多以透镜体形式夹杂于蛇纹岩和变杂砂岩中, 且仅占小部分, 这与Chen等(2013)大洋榴辉岩浮力折返模型及自然观察不完全符合. 通过洋壳榴辉岩的相平衡和热力学模拟, Wang Y等(2019)发现硬柱石榴辉岩能通过自身浮力折返, 且自折返深度随上覆岩石圈厚度增加而增加, 而绝大多数绿帘石榴辉岩折返则需要借助其他低密度岩石(如蛇纹岩、变沉积岩等)(图7). Chen等(2013)与Wang Y等(2019)相平衡模拟采用的洋壳成分略有不同, 密度计算方法也不相同, 前者得出的密度差$\Delta\rho$=0曲线位置比后者高约50~100℃, 但是, 其共同点是: 在低温低压-中温高压区域, 俯冲洋壳均受正浮力的作用. 因此, 大洋成因榴辉岩折返过程中可能受自身正浮力影响, 但仍需要更多自然大洋成因榴辉岩样品的进一步验证.

4.2　外部驱动力

俯冲地壳折返过程中存在内摩擦阻力. 浮力可能是俯冲地壳折返的必要、但不充分条件(Gerya等, 2002; Beaumont等, 2009). 如上所述, Wang Y等(2019)表明部分洋壳榴辉岩能够借助自身浮力折返, 但进一

步地球动力学模拟发现如果不加入蛇纹岩和变沉积岩, 洋壳榴辉岩不能沿俯冲隧道折返, 因此认为其折返不仅取决于密度差, 与流变性阻力也有关系. 前人提出其他作用力对俯冲地壳折返的作用, 包括角流、回流或隧道流(Shreve和Cloos, 1986; Beaumont等, 2001; Gerya等, 2002; 郑永飞等, 2013), 以及挤出作用内部热的或软弱物质被挤出(Warren等, 2008b; Warren, 2013). Beaumont等(2001)指出, 地表剥蚀作用结合中下隧道流韧性挤出可能引起喜马拉雅俯冲陆壳折返. 隧道流模型强调俯冲板片和上覆板片之间的黏滞力, 引起软弱物质环流或涡流(Shreve和Cloos, 1986; Gerya等, 2002).

宇宙成因核素和热年代学表明, 剥蚀速率一般在μm a^{-1}, 极少数可以达到mm a^{-1}, 但不太可能持续上百万年(Burbank, 2002). PNG柯石英榴辉岩折返速率达到cm a^{-1}, 且缺乏造山作用叠加(Gordon等, 2012), 因此剥蚀作用对其折返影响可以忽略. 大洋俯冲带位于海平面之下, 缺乏风化剥蚀作用, 因此洋壳折返受剥蚀作用影响也可以忽略. 此外, 碰撞造山带周缘盆地中很少有同折返沉积岩报道. 因此从地幔深度折返至地壳水平, 剥蚀对俯冲陆壳折返作用有限(Yamato等, 2008). Platt(1993)指出, 如果风化剥蚀作用是折返的唯一因素, 部分超高压变质岩围岩应该来自下地壳岩石和地幔, 这些围岩部分经历剥蚀形成同折返沉积岩, 然而尚未发现这样的超高压变质岩围岩. 剥蚀作用可能对俯冲地壳从中-下地壳出露至地表具有重要作用(Warren, 2013). 数值模拟也表明高压-超高压变质岩能够借助板片后撤(Husson等, 2009)或上盘远离海沟/增生楔运移(Liao等, 2018)等快速折返至地表, 无需剥蚀作用协助. Yan和Zhang(2019)发现全球超高压变质岩出露位置总是位于南北纬30°之间, 因此认为俯冲地壳折返与剥蚀作用和气候有关.

5 深俯冲地壳折返的地球动力学背景

俯冲带构造应力状态对俯冲板片与上盘界面解耦和耦合以及折返方式具有至关重要的作用, 然而这种影响却常被忽视, 如俯冲隧道模型常用来解释俯冲地壳折返, 但折返的构造动力学背景, 仍缺乏深入讨论和存在争议. 先前众多模型设定海沟位置固定不变(Chemenda等, 1995; Ernst等, 1997), 然而汇聚板块边缘岛弧和海沟常随时间而迁移(Schellart等, 2008). 大洋俯冲带一般分为海沟前进的挤压型、海沟后撤的拉张型和海沟位置不变的过渡型. 以Indo-Atlantic热点(hotspot)为参考, 75%海沟属于后撤型(Schellart等, 2008). 尽管大陆俯冲带资料相对匮乏, 但仍然识别出了类似的后撤型和前进型(Liao等, 2017). 因此, 由于板片在俯冲过程中相对上盘前进或后退(Liao等, 2017), 以及地壳内部存在多个低黏度带(Meissner和Mooney, 1998)和俯冲地壳内部的多层次拆离解耦(Liu等, 2007b; 刘贻灿和李曙光, 2008; 郑永飞等, 2013), 俯冲地壳岩石的折返可能存在伸展和挤压两种构造动力学背景或应力状态(stress state), 但是, 它们可能发生于不同的俯冲-碰撞阶段, 并随时间的演化而发生转变(Horton和Fuentes, 2016; Yamato和Brun, 2017; Chu等, 2019). 由于板片汇聚, 地壳俯冲早期处于挤压应力状态, 常在浅部发生地壳拆离解耦和折返, 如大别山(Zheng等, 2005; 刘贻灿和李曙光, 2008; Liu等, 2017)和苏鲁(Tang等, 2006)等造山带.

目前, 自然界的高压-超高压岩石折返可能大多数发生在伸展构造背景条件下(Andersen等, 1991; Brun和Faccenna, 2008; Duretz等, 2016). Yamato和Brun(2017)根据力学分析发现, 高压-超高压变质岩的峰期压力也许并不一定反映最大俯冲深度, 而与退变质早期的压力降低量成正比, 而且, 证明这与俯冲时的挤压向折返初期的伸展环境下的应力状态快速转变有关并提供了(超)高压岩石变质*P-T-t*轨迹中观察到的峰期之后突然地快速、近于等温减压过程的一个简单的物理解释, 因而认为超高压变质岩的折返发生在伸展背景下. 然而, Hodges(2017)认为该模型目前尚缺乏超高压岩石达到最大俯冲深度之后的极端快速减压的岩石学方面证据, 还需要进一步的实验和野外地质方面研究证据予以支撑. Chemenda等(1995)通过类比实验发现, 挤压和剥蚀作用会引起俯冲地壳拆离折返, 当剥蚀作用停止时, 俯冲地壳无法显著折返. 因此, 尽管仍存在一些问题和争议, 但上述资料可能暗示俯冲地壳岩石在处于伸展应力状态下才能折返.

根据俯冲地壳折返动力学机制差异, 伸展背景条件下的折返至少包含五种类型. 第一种类型, 数值模拟和GPS观测等表明, 随着俯冲带成熟, 部分俯冲板片回转(Schellart, 2004; Stegman等, 2006; Gonzalez-Castillo等, 2015), 如马里亚纳大洋型俯冲带(Tamblyn等,

2019)和亚平宁大陆型俯冲带(Faccenda等, 2009). 海沟后撤越快, 俯冲角度越大, 板片折返越快(Brun和Faccenna, 2008). 而海沟迁移与俯冲板片年龄、厚度、速率和强度等有关(Stegman等, 2006; Agrusta等, 2017). 数值模拟表明, 年龄较老、厚度较大的俯冲板块容易形成海沟后撤型俯冲(周信等, 2019). 第二种类型, 上盘远离海沟运移(divergence)形成相对伸展的构造环境, 俯冲地壳伸展折返(图8)(Malusà等, 2011, 2015; Liao等, 2018), 并可能促使地幔楔折返(Solarino等, 2018). 板片后撤模型与上盘相对海沟/增生楔远离模型区别在于, 前者引起高压-超高压变质岩就位于俯冲下盘边界, 靠近下盘峰期变质年龄有变年轻趋势, 且沉积于海沟的浊积岩易于被刮铲下来或进入俯冲带; 而后者促进折返岩石就位于上盘边界(图8), 靠近上盘峰期变质年龄有变年轻趋势, 浊积岩通常缺乏变质作用, 只是发生轻微变形(Malusà等, 2011, 2015). 此外, 俯冲过程中板片发生旋转伸展也有利于高压-超高压变质岩快速折返(Webb等, 2008; Bottrill等, 2014). 第三种类型, 当上盘发生碰撞后板内伸展作用, 一方面超高压变质岩与周围地幔岩石相比, 强度相对低, 导致在其上方发生局部裂解; 另一方面板内伸展作用也降低了局部裂解的岩石圈有效黏度, 引起超高压变质岩减压熔融和底辟折返(Ellis等, 2011). 第四种类型, 板片断离引起造山带伸展垮塌, 俯冲地壳快速折返(图1a), 如上述挪威加里东造山带(Andersen等, 1991; Duretz等, 2012). 第五种类型, 靠近老的大陆碰撞带, 形成新的大洋型俯冲带, 原俯冲带上盘转变为新俯冲带下盘引起区域伸展和超高压变质岩折返(Petersen和Buck, 2015).

此外, 伸展背景条件下的折返, 常伴随地壳减薄(Leech, 2001; Faccenda等, 2009), 造山带内部会发育伸展构造(如伸展盆地)(Andersen等, 1991; Faccenda等, 2009; Tamblyn等, 2019), 并可能出现软流圈地幔上涌、拆沉作用、地壳隧道流和高原形成(Beaumont等, 2001; Göğüş和Pysklywec, 2008; Gray和Pysklywec, 2012; Liao等, 2018), 引起俯冲带P/T比值降低, 岩浆活动相对发育(Faccenda等, 2009; Gordon等, 2012; Palmer等, 2019), 折返速率很高(~cm a^{-1})(Brun和Faccenna, 2008; Malusà等, 2011; Duretz等, 2012; Gordon等, 2012; Warren, 2013; Bottrill等, 2014). 因此, 伸展背景条件下, 可能更有利于俯冲地壳岩石的折返(Faccenda等, 2009; Malusà等, 2011, 2015; Duretz等, 2012; Liao等, 2018).

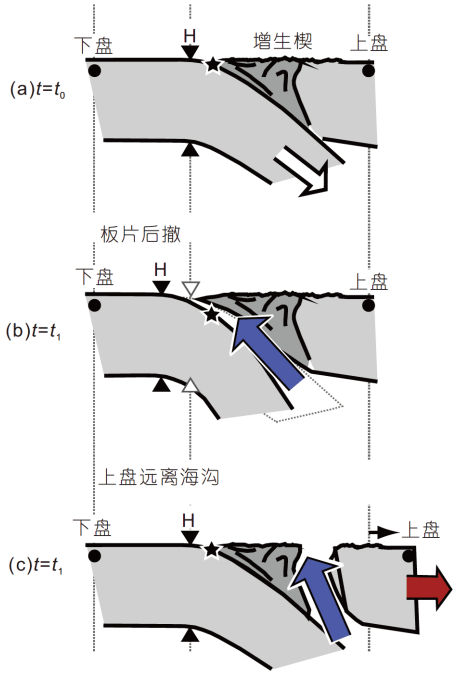


图 8　板片后撤模型与上盘远离海沟/增生楔运移模型之间的差异示意图

(a) 折返前的俯冲带; (b) 板片后撤, 高压-超高压变质岩就位于俯冲下盘边界, 浊积岩进入俯冲隧道; (c) 俯冲带上盘远离海沟运移, 折返岩石就位于上盘边界. H代表俯冲铰链, 实心三角代表上盘和下盘固定位置的参考点, 而五角星代表t_0时沉积海沟处的浊积岩. 修改自Malusà等(2011)

6　展望

深俯冲地壳的折返机制是地球动力学的基本问题之一. 俯冲地壳折返既受地壳浅部作用影响, 也受地幔作用控制. 俯冲带构造应力、热结构以及上下盘接触界面时空演化控制着俯冲地壳岩石的变质作用、变形作用、部分熔融作用和拆离解耦, 进而影响俯冲地壳的折返. 折返板片内部不同的地质过程可能对应不同的折返机制, 因此, 进一步理清地壳俯冲和折返期间内部地质过程是研究俯冲地壳折返机制的先决条件. 此外, 探讨俯冲地壳折返与浅部和地幔之间的相互作用也是非常重要的.

6.1　折返地壳内部的地质过程

经历了不同折返过程而出露的高压-超高压变质岩, 常具有多种多样的地质演化历史和截然不同的变质P-T-t轨迹. 目前存在的主要问题如下.

(1) 折返地壳的初始状态如流体含量、密度和深度与原岩性质和俯冲过程有关. 与退变质作用相比, 前进变质作用的地质记录相对较少, 进而不易恢复俯冲过程, 需要更多定量化工作.

(2) 变质*P-T-t*轨迹的重建还存在一些问题(Massonne, 2013; Lanari和Engi, 2017; 吴春明, 2018). 例如, 造山带橄榄岩记录了俯冲带地幔动力学过程, 但恢复其变质条件并不容易(陈意等, 2015; Su等, 2019). 此外, 对高温(>850℃)变质作用的时间和峰期温度确定也有一定困难(刘贻灿等, 2015). 最近, 部分大陆俯冲带发现了高温超高压变质作用, 如北大别高温超高压变质带峰期变质温度大于900℃(Liu等, 2015), 哈萨克斯坦Kokchetav地体(Schertl和Sobolev, 2013)和南阿尔金(Dong等, 2018)陆壳深俯冲最高变质温度大于1000℃. 然而, 鉴于高温条件下绝大多数同位素体系是开放的(Liu等, 2011), 因此高温超高压变质岩时间的准确限定还有待于进一步解决.

(3) 变质不均一性. 目前, 在不同造山带中, 同一变质带不同岩石往往记录了不同的峰期变质条件, 这一现象带来了很大的构造演化争议. 超高压变质带低级变质岩和榴辉岩相变质岩广泛共存(Dong等, 1997; 刘贻灿等, 2013; Li和Massonne, 2017; Li等, 2020b), 这些浅变质岩与高压-超高压变质岩之间的成因联系和相互关系是地质学家长期争论的焦点(Proyer, 2003; Bousquet, 2008; 姜为佳和刘贻灿, 2016; Brueckner, 2018).

(4) 俯冲带热温度结构模型与岩石记录之间差异的原因(Penniston-Dorland等, 2015; van Keken等, 2018), 以及造山带中大量的低温-超高压变质岩石如何形成和保存的(Chemenda等, 1997, 2001; Boutelier和Chemenda, 2008).

(5) 折返期间退变质作用、脱水作用和深熔作用过程及其地球动力学效应, 熔流体地球化学行为有待进一步深入. 例如, 地壳折返过程中常伴随不同程度的部分熔融(Rosenberg, 2001; Labrousse等, 2015; 刘贻灿等, 2015; Chen等, 2017; Deng等, 2018), 实验和数值模拟证据表明, 深熔作用对俯冲地壳折返具有重要的地球动力学效应, 然而目前关键的自然样品证据仍然缺乏. 另外, 俯冲-折返过程中变超镁铁质岩能否发生部分熔融作用, 仍然缺乏系统深入研究.

(6) 俯冲板片断离的机制与效应认识仍非常有限. 关于板片断离, 前人进行了大量观测、类比实验和数值模拟(Wortel和Spakman, 2000; Buiter等, 2002; Li等, 2002; Neubauer等, 2005; Duretz等, 2011; van Hunen和Allen, 2011; Boutelier和Cruden, 2017; Pusok等, 2018), 提出了板片断离的不同机制(Gerya等, 2004; Duretz等, 2011, 2012). 然而类比模型中, 模拟材料的流变性很少反映真实的岩石圈地幔流变学特征(Broerse等, 2019). 不同数值模型流变学估算不同, 之间很难相互对比(Pusok等, 2018). 俯冲地壳断离机制是什么? 为什么仅部分造山带经历了板片断离(Garzanti等, 2018)? 此外, 板片断离常被用来解释许多事件, 包括岩浆爆发、快速地表隆升、沉积物供应加快、变质岩快速折返等(Garzanti等, 2018). 板片断离模型常常用来初步解释一些知之甚少的观测, 部分犯了循环论证的错误(Garzanti等, 2018). 因此, 上述现象与板片断离之间的关系和成因联系有待进一步研究.

(7) 同碰撞岩浆作用与陆壳净生长关系. Niu等(2013)以冈底斯造山带为例, 认为在大陆碰撞过程中有显著地壳生长. 但是, Zheng(2012)和Zheng等(2019)以大别-苏鲁造山带为例, 认为大陆碰撞过程中只有汇聚板块边缘华南和华北陆块地壳的再造, 没有新生地壳生长. 对这两种认识争论的焦点在于, 相对亏损Nd-Hf同位素组成的长英质火成岩具有何种成因.

6.2 俯冲地壳折返-地表过程相互作用

地表过程对俯冲地壳的折返具有一定作用(Wang和Cong, 1999; Beaumont等, 2001; Behr和Becker, 2018; Yan和Zhang, 2019), 反之, 俯冲地壳折返影响地壳环境、气候(刘静等, 2018)、地形(Duretz等, 2011)、成矿(Chen等, 2019)和生命活动等. 地表过程一方面影响最终地壳折返过程中去顶作用(Warren, 2013), 还影响俯冲开始前板块边缘沉积物含量. 沉积物能够润滑俯冲隧道(Sobolev和Brown, 2019), 其相对比例影响俯冲隧道的黏度, 因而控制板块俯冲速率(Behr和Becker, 2018; Sobolev和Brown, 2019), 影响俯冲隧道的宽度(Ichikawa等, 2015). 沉积物通量在不同造山带和造山阶段可能均有差异(Behr和Becker, 2018). Yan和Zhang(2019)基于超高压变质岩的空间分布, 指出折返受气候控制, 折返的超高压变质岩或许能作为古环境的指示. 此外, 冰川剥蚀速率的提高能够加速俯冲地壳的抬升和折返(Jiao等, 2017). 但是, 构造与地表抬升、剥

蚀作用和气候之间的相互作用存在很多争论(Whipple, 2014; Jiao等, 2017). 以构造-气候-地表过程相互作用为核心的构造地貌学已经成为地球科学领域新兴的热点研究方向之一(刘静等, 2018). 有关地表过程-俯冲地壳折返相互作用的定量分析比较缺乏.

俯冲地壳的拆离折返暗示俯冲带构造体制可能发生了转变, 可能有利于成矿. 已有研究表明, 俯冲-碰撞造山带是重要的成矿系统(张洪瑞和侯增谦, 2018). 一方面超高压变质岩可能是潜在矿床, 或能够提供成矿物质. 例如, 前人发现了大量的榴辉岩型金红石矿床(Chen等, 2019). 另一方面, 超高压变质岩折返期间可能成矿. 此外, 造山隆升驱动的盆地流体也可能提供了成矿物质来源(毕献武等, 2019), 以及超高压变质岩折返常就位于变质穹窿构造中心(Beaumont等, 2009). 变质穹窿能够提供高的地温梯度和断裂, 因此影响金属运移和成矿(Menant等, 2018). 折返期间周缘盆地会形成巨厚层碎屑沉积(Yang等, 2010; 刘少峰和张国伟, 2013), 可能富含油气资源. 目前, 与深俯冲地壳折返相关的成矿作用尚缺乏深入认识.

6.3 俯冲地壳折返-地幔相互作用

深地探测揭示了地球精细的圈层构造及垂向和横向上不均匀性(傅容珊等, 2012). 这些结果深化了人们对地球深部的认识, 同时也滋生出新的地球动力学问题, 如不同圈层结构对深俯冲地壳演化的影响(Funiciello等, 2003, 2004; Yoshida, 2017). 此外, 圈层内部物质运移、不同圈层对流、板块俯冲和折返可以看成是统一的地球动力学系统. 例如, 大洋岩石圈俯冲进入地幔过渡带, 与地幔相互作用, 发育了不同的俯冲板片几何形态(Goes等, 2017), 进而影响俯冲板片的动力学行为和海沟的运动模式. 周信等(2019)对俯冲板片上地幔动力学进行了系列数值模拟. 他们的结果显示, 俯冲板片与地幔转换带相互作用, 形成了三种海沟迁移模式. 这些不同几何形态的板片和不同类型的海沟迁移模式可能对俯冲板片动力学具有重要影响(Schellart, 2004; Brun和Faccenna, 2008). 阿尔金超高压变质带中变沉积岩的岩石学研究表明, 陆壳可能俯冲到>350km地幔深度并折返至地表(Liu L等, 2007); 然而, 它超出了由实验限定的俯冲上陆壳的最大折返深度(250km)(Wu等, 2009). 据此, 推测超深俯冲陆壳折返可能受俯冲板片与深部地幔相互作用而折返, 但仍需要进一步查证.

此外, 板片折返可能反过来影响上盘地幔楔的地球化学特征. 而且, 俯冲地壳与上覆地幔楔之间发生相互作用, 造成地幔楔水化, 有利于俯冲隧道宽度增加, 从而促进俯冲地壳沿隧道折返. 另一方面, 当地壳沿俯冲带折返, 折返地壳会成为俯冲地壳和上覆地幔楔之间的物理屏障, 可能阻碍俯冲板片与上覆地幔楔进一步相互作用, 但高压-超高压变质岩在折返过程中出现脱水和深熔作用, 从而发生折返板片与地幔相互作用. Massonne(2012)基于岩石学观测, 最早提出了“折返隧道”概念, 认为榴辉岩先在俯冲隧道中向上快速折返, 之后在折返隧道中基本近水平慢速折返, 折返隧道中的物质相对软、湿和冷. 类比“俯冲隧道”模型(Shreve和Cloos, 1986; Gerya等, 2002; 郑永飞等, 2013), 我们引入并扩展“折返隧道”概念, 将俯冲带中正在折返的物质与上盘之间的剪切带称为统称为“折返隧道”, 强调折返物质与上盘之间的相互作用, 主要是考虑到折返过程并不是板片俯冲过程的简单逆过程, 主要表现在: (1) 折返隧道与俯冲隧道物理化学性质不同. 板片俯冲起始阶段和折返阶段岩石性质和组合明显不同. (2) 热结构可能不同. 折返隧道地温梯度常常比俯冲隧道高. (3) 折返隧道和俯冲隧道动力学体制可能不同. 折返初始可能发生板片断离、板片后撤、板片旋转等重大地质事件, 影响动力学体制. “折返隧道”概念引入并扩展有利于进一步深化对壳-幔相互作用过程、折返过程和机制的理解.

然而, “折返隧道”涉及如下科学问题: (1) 折返隧道和俯冲隧道有什么空间和成因联系? (2) 折返物质-地幔相互作用与俯冲物质-地幔相互作用之间有什么区别? (3) 流体迁移路径与折返隧道的空间关系? Wang H L等(2019)数值模拟发现, 俯冲带板片脱水流体有两种迁移路径, 包括向海沟方向(trench-ward)和岛弧方向迁移(arc-ward). 正如前文所述, 俯冲地壳折返轨迹也有两种: 沿隧道折返和底辟折返. 由此表明, 俯冲带流体迁移路径和俯冲板片折返轨迹相吻合, 而且, 俯冲地壳折返轨迹受流体迁移路径所控制, 流体可以看作是最基本的折返物质, 因此, 我们或许通过探测流体的迁移路径来示踪超高压变质岩的折返轨迹. (4) “折返隧道”是连续的还是间断的? Agard等(2009)发现洋壳(+地幔)折返时间是短期的、不连续的. 因此这种不连续性可能导致折返地壳与地幔楔相互作用是幕式

的, 但仍有待于进一步验证.

综上所述, 恢复深俯冲地壳的折返过程和探讨对应的地球动力学机制是一个系统工程. 碰撞造山带常因先后经历了不同的构造动力学背景和多阶段变质演化与改造, 形成一系列断裂控制的构造岩石单位甚至构造混杂岩带(徐树桐等, 2008; 刘贻灿等, 2013), 高压-超高压变质岩石中常常形成多阶段矿物组合和单矿物可能形成复杂的成分环带. 因此, 需要提升单矿物元素和同位素原位微区分析测试技术的精度和研制三维原子探针. 而且, 关键的高温高压实验仪器、原位地球化学分析技术和模拟计算方法的开发和应用将有助于进一步深化深俯冲地壳折返过程和机制的认识.

致谢　感谢主编郑永飞院士的约稿和建设性修改意见, 以及张立飞教授和三位匿名审稿人提出的宝贵意见. 感谢胡子安同学在参考文献方面提供的帮助.

参考文献

毕献武, 唐永永, 陶琰, 王长明, 胥磊落, 戚华文, 兰青, 木兰. 2019. 西南三江碰撞造山带沉积岩容矿Pb-Zn-Ag-Cu贱金属复合成矿与深部过程. 岩石学报, 35: 1341–1371

陈意, 苏斌, 郭顺. 2015. 大别-苏鲁造山带橄榄岩: 进展和问题. 中国科学: 地球科学, 45: 1245–1269

陈意, 叶凯. 2013. 俯冲洋壳的折返及其相关问题讨论. 岩石学报, 29: 1461–1478

傅容珊, 黄建华, 杨亭. 2012. 地球深内部探测及动力学研究. 大地测量与地球动力学, 32: 139–151, 159

姜为佳, 刘贻灿. 2016. 超高压变质带中的变质不均一性. 地球科学与环境学报, 38: 160–171

李忠海. 2014. 大陆俯冲-碰撞-折返的动力学数值模拟研究综述. 中国科学: 地球科学, 44: 817–843

李曙光, 李秋立, 侯振辉, 杨蔚, 王莹. 2005. 大别山超高压变质岩的冷却史及折返机制. 岩石学报, 21: 1117–1124

刘静, 张金玉, 葛玉魁, 王伟, 曾令森, 李根, 林旭. 2018. 构造地貌学: 构造-气候-地表过程相互作用的交叉研究. 科学通报, 63: 3070–3088

刘少峰, 张国伟. 2013. 大别造山带周缘盆地发育及其对碰撞造山过程的指示. 科学通报, 58: 1–26

刘贻灿, 李曙光. 2005. 大别山下地壳岩石及其深俯冲. 岩石学报, 21: 1059–1066

刘贻灿, 李曙光. 2008. 俯冲陆壳内部的拆离和超高压岩石的多板片差异折返: 以大别-苏鲁造山带为例. 科学通报, 53: 2153–2165

刘贻灿, 李远, 刘理湘, 古晓峰, 邓亮鹏, 刘佳. 2013. 大别造山带三叠纪低级变质的新元古代火成岩: 俯冲陆壳表层拆离折返的岩片. 科学通报, 58: 2330–2337

刘贻灿, 邓亮鹏, 古晓锋. 2015. 大陆俯冲碰撞带高温超高压变质岩的多阶段折返与部分熔融. 中国科学: 地球科学, 45: 752–769

吴春明. 2018. 变质地质学研究中的一些困难问题. 岩石学报, 34: 873–894

徐树桐, 吴维平, 刘贻灿, 王华明. 2008. 大别山的变质碰撞混杂岩——以东部为例. 地质力学学报, 14: 1–21

杨建平, 金振民, 欧新功, 徐海军. 2005. 岩石密度和超高压岩石折返速率. 岩石学报, 2: 427–437

杨经绥, 许志琴, 张建新, 张泽明, 刘福来, 吴才来. 2009. 中国主要高压-超高压变质带的大地构造背景及俯冲/折返机制的探讨. 岩石学报, 25: 1529–1560

张洪瑞, 侯增谦. 2018. 大陆碰撞带成矿作用: 年轻碰撞造山带对比研究. 中国科学: 地球科学, 48: 1629–1654

张立飞, 吕增, 张贵宾, 宋述光. 2008. 大洋型超高压变质带的地质特征及其研究意义: 以西南天山、柴北缘超高压变质带为例. 科学通报, 18: 2166–2175

张立飞, 王杨. 2020. 俯冲带高压-超高压变质地体的抬升折返机制: 问题和探讨. 中国科学: 地球科学, doi: 10.1360/SSTe-2020-0002

郑永飞, 赵子福, 陈伊翔. 2013. 大陆俯冲隧道过程:大陆碰撞过程中的板块界面相互作用. 科学通报, 58: 2233–2239

郑永飞, 陈仁旭, 徐峥, 张少兵. 2016. 俯冲带中的水迁移. 中国科学: 地球科学, 46: 253–286

周信, 许志琴, 李忠海, 皇甫鹏鹏, 张进江. 2019. 上地幔俯冲板块的动力学过程: 数值模拟. 地球物理学报, 62: 2455–2465

Abers G A, Nakajima J, van Keken P E, Kita S, Hacker B R. 2013. Thermal-petrological controls on the location of earthquakes within subducting plates. Earth Planet Sci Lett, 369-370: 178–187

Abers G A, van Keken P E, Kneller E A, Ferris A, Stachnik J C. 2006. The thermal structure of subduction zones constrained by seismic imaging: Implications for slab dehydration and wedge flow. Earth Planet Sci Lett, 241: 387–397

Agard P, Plunder A, Angiboust S, Bonnet G, Ruh J. 2018. The subduction plate interface: Rock record and mechanical coupling (from long to short timescales). Lithos, 320-321: 537–566

Agard P, Searle M P, Alsop G I, Dubacq B. 2010. Crustal stacking and expulsion tectonics during continental subduction: *P-T* deformation constraints from Oman. Tectonics, 29: TC5018

Agard P, Yamato P, Jolivet L, Burov E. 2009. Exhumation of oceanic blueschists and eclogites in subduction zones: Timing and mechanisms. Earth-Sci Rev, 92: 53–79

Agrusta R, Goes S, van Hunen J. 2017. Subducting-slab transition-zone interaction: Stagnation, penetration and mode switches. Earth Planet Sci Lett, 464: 10–23

Andersen T B, Jamtveit B, Dewey J F, Swensson E. 1991. Subduction

and eduction of continental crust: Major mechanisms during continent-continent collision and orogenic extensional collapse, a model based on the south Norwegian Caledonides. Terra Nova, 3: 303–310

Angiboust S, Hyppolito T, Glodny J, Cambeses A, Garcia-Casco A, Calderón M, Juliani C. 2017. Hot subduction in the middle Jurassic and partial melting of oceanic crust in Chilean Patagonia. Gondwana Res, 42: 104–125

Aoki I, Takahashi E. 2004. Density of MORB eclogite in the upper mantle. Phys Earth Planet Inter, 143-144: 129–143

Auzanneau E, Vielzeuf D, Schmidt M W. 2006. Experimental evidence of decompression melting during exhumation of subducted continental crust. Contrib Mineral Petrol, 152: 125–148

Baldwin S L, Monteleone B D, Webb L E, Fitzgerald P G, Grove M, June Hill E. 2004. Pliocene eclogite exhumation at plate tectonic rates in eastern Papua New Guinea. Nature, 431: 263–267

Baumann C, Gerya T V, Connolly J A D. 2010. Numerical modelling of spontaneous slab breakoff dynamics during continental collision. Geol Soc Lond Spec Publ, 332: 99–114

Beaumont C, Jamieson R A, Butler J P, Warren C J. 2009. Crustal structure: A key constraint on the mechanism of ultra-high-pressure rock exhumation. Earth Planet Sci Lett, 287: 116–129

Beaumont C, Jamieson R A, Nguyen M H, Lee B. 2001. Himalayan tectonics explained by extrusion of a low-viscosity crustal channel coupled to focused surface denudation. Nature, 414: 738–742

Behn M D, Kelemen P B, Hirth G, Hacker B R, Massonne H J. 2011. Diapirs as the source of the sediment signature in arc lavas. Nat Geosci, 4: 641–646

Behr W M, Becker T W. 2018. Sediment control on subduction plate speeds. Earth Planet Sci Lett, 502: 166–173

Bercovici D, Schubert G, Ricard Y. 2015. Abrupt tectonics and rapid slab detachment with grain damage. Proc Natl Acad Sci USA, 112: 1287–1291

Bottrill A D, van Hunen J, Cuthbert S J, Brueckner H K, Allen M B. 2014. Plate rotation during continental collision and its relationship with the exhumation of UHP metamorphic terranes: Application to the Norwegian Caledonides. Geochem Geophys Geosyst, 15: 1766–1782

Bousquet R. 2008. Metamorphic heterogeneities within a single HP unit: Overprint effect or metamorphic mix? Lithos, 103: 46–69

Boutelier D, Cruden A R. 2017. Slab breakoff: Insights from 3D thermo-mechanical analogue modelling experiments. Tectonophysics, 694: 197–213

Boutelier D A, Chemenda A I. 2008. Exhumation of UHP/LT rocks due to the local reduction of the interplate pressure: Thermo-mechanical physical modelling. Earth Planet Sci Lett, 271: 226–232

Broerse T, Norder B, Govers R, Sokoutis D, Willingshofer E, Picken S J. 2019. New analogue materials for nonlinear lithosphere rheology, with an application to slab break-off. Tectonophysics, 756: 73–96

Brown M. 2006. Duality of thermal regimes is the distinctive characteristic of plate tectonics since the Neoarchean. Geology, 34: 961–964

Brown M, Johnson T. 2019. Metamorphism and the evolution of subduction on Earth. Am Miner, 104: 1065–1082

Brueckner H K. 2018. The great eclogite debate of the Western Gneiss Region, Norwegian Caledonides: The *in situ* crustal *v*. exotic mantle origin controversy. J Metamorph Geol, 36: 517–527

Brun J P, Faccenna C. 2008. Exhumation of high-pressure rocks driven by slab rollback. Earth Planet Sci Lett, 272: 1–7

Buiter S J H, Govers R, Wortel M J R. 2002. Two-dimensional simulations of surface deformation caused by slab detachment. Tectonophysics, 354: 195–210

Burbank D W. 2002. Rates of erosion and their implications for exhumation. Mineral Mag, 66: 25–52

Burov E, Francois T, Yamato P, Wolf S. 2014a. Mechanisms of continental subduction and exhumation of HP and UHP rocks. Gondwana Res, 25: 464–493

Burov E, Francois T, Agard P, Le Pourhiet L, Meyer B, Tirel C, Lebedev S, Yamato P, Brun J P. 2014b. Rheological and geodynamic controls on the mechanisms of subduction and HP/UHP exhumation of crustal rocks during continental collision: Insights from numerical models. Tectonophysics, 631: 212–250

Burov E, Jolivet L, Le Pourhiet L, Poliakov A. 2001. A thermo-mechanical model of exhumation of high pressure (HP) and ultra-high pressure (UHP) metamorphic rocks in Alpine-type collision belts. Tectonophysics, 342: 113–136

Burov E, Yamato P. 2008. Continental plate collision, *P-T-t-z* conditions and unstable vs. stable plate dynamics: Insights from thermo-mechanical modelling. Lithos, 103: 178–204

Butler J P, Beaumont C, Jamieson R A. 2011. Crustal emplacement of exhuming (ultra)high-pressure rocks: Will that be pro- or retro-side? Geology, 39: 635–638

Carry N, Gueydan F, Brun J P, Marquer D. 2009. Mechanical decoupling of high-pressure crustal units during continental subduction. Earth Planet Sci Lett, 278: 13–25

Castro A, Gerya T V. 2008. Magmatic implications of mantle wedge plumes: Experimental study. Lithos, 103: 138–148

Chapman T, Clarke G L, Daczko N R. 2019. The role of buoyancy in the fate of ultra-high-pressure eclogite. Sci Rep, 9: 19925

Chatterjee N, Jagoutz O. 2015. Exhumation of the UHP Tso Morari eclogite as a diapir rising through the mantle wedge. Contrib Mineral Petrol, 169: 3

Chemenda A I, Hurpin D, Tang J C, Stephan J F, Buffet G. 2001. Impact of arc-continent collision on the conditions of burial and exhumation of UHP/LT rocks: Experimental and numerical modelling. Tectonophysics, 342: 137–161

Chemenda A I, Mattauer M, Bokun A N. 1996. Continental subduction and a mechanism for exhumation of high-pressure metamorphic rocks: New modelling and field data from Oman. Earth Planet Sci Lett, 143: 173–182

Chemenda A I, Mattauer M, Malavieille J, Bokun A N. 1995. A mechanism for syn-collisional rock exhumation and associated normal faulting: Results from physical modelling. Earth Planet Sci Lett, 132: 225–232

Chemenda A, Matte P, Sokolov V. 1997. A model of Palaeozoic obduction and exhumation of high-pressure/low-temperature rocks in the southern Urals. Tectonophysics, 276: 217–227

Chen X, Xu R K, Zheng Y Y, Gao S B, Cai P J, Yu J Z, Wang Q M. 2019. The geodynamic setting of Dulan eclogite-type rutile deposits in the North Qaidam orogen, western China. Ore Geol Rev, 110: 102936

Chen Y, Ye K, Wu T F, Guo S. 2013. Exhumation of oceanic eclogites: Thermodynamic constraints on pressure, temperature, bulk composition and density. J Meta Geol, 31: 549–570

Chen Y, Li W, Yuan X, Badal J, Teng J. 2015. Tearing of the Indian lithospheric slab beneath southern Tibet revealed by SKS-wave splitting measurements. Earth Planet Sci Lett, 413: 13–24

Chen Y X, Zhou K, Gao X Y. 2017. Partial melting of ultrahigh-pressure metamorphic rocks during continental collision: Evidence, time, mechanism, and effect. J Asian Earth Sci, 145: 177–191

Chopin C. 1984. Coesite and pure pyrope in high-grade blueschists of the Western Alps: A first record and some consequences. Contr Mineral Petrol, 86: 107–118

Chopin C, Schertl H P. 1999. The UHP unit in the Dora-Maira Massif, western Alps. Int Geol Rev, 41: 765–780

Chu Y, Lin W, Faure M, Xue Z H, Ji W B, Feng Z T. 2019. Cretaceous episodic extension in the South China Block, East Asia: Evidence from the Yuechengling massif of central South China. Tectonics, 38: 3675–3702

Cloos M, Shreve R L. 1988. Subduction-channel model of prism accretion, melange formation, sediment subduction, and subduction erosion at convergent plate margins: 2. Implications and discussion. Pure Appl Geophys, 128: 501–545

Currie C A, Beaumont C, Huismans R S. 2007. The fate of subducted sediments: A case for backarc intrusion and underplating. Geology, 35: 1111–1114

Cutts J A, Smit M A, Kooijman E, Schmitt M. 2019. Two-stage cooling and exhumation of deeply subducted continents. Tectonics, 38: 863–877

Davies J H, von Blanckenburg F. 1995. Slab breakoff: A model of lithosphere detachment and its test in the magmatism and deformation of collisional orogens. Earth Planet Sci Lett, 129: 85–102

De Franco R, Govers R, Wortel R. 2006. Numerical comparison of different convergent plate contacts: Subduction channel and subduction fault. Geophys J Int, 171: 435–450

Defant M J, Drummond M S. 1990. Derivation of some modern arc magmas by melting of young subducted lithosphere. Nature, 347: 662–665

Deng L P, Liu Y C, Gu X F, Groppo C, Rolfo F. 2018. Partial melting of ultrahigh-pressure metamorphic rocks at convergent continental margins: Evidences, melt compositions and physical effects. Geosci Front, 9: 1229–1242

Deng L P, Liu Y C, Yang Y, Groppo C, Rolfo F, Gu X F. 2019. Anatexis of high-*T* eclogites in the Dabie orogen triggered by exhumation and post-orogenic collapse. Eur J Mineral, 31: 889–903

Deschamps F, Godard M, Guillot S, Hattori K. 2013. Geochemistry of subduction zone serpentinites: A review. Lithos, 178: 96–127

Dong J, Wei C J, Clarke G L, Zhang J X. 2018. Metamorphic evolution during deep subduction and exhumation of continental crust: Insights from felsic granulites in South Altyn Tagh, West China. J Petrol, 59: 1965–1990

Dong S W, Wang X F, Huang D Z. 1997. Discovery of low grade metamorphic volcanic rock sheets within UHP in Dabie Mts. and its implications. Chin Sci Bull, 42: 1199–1203

Ducea M N. 2016. Research focus: Understanding continental subduction: A work in progress. Geology, 44: 239–240

Duchêne S, Lardeaux J M, Albarède F. 1997. Exhumation of eclogites: Insights from depth-time path analysis. Tectonophysics, 280: 125–140

Duretz T, Gerya T V, May D A. 2011. Numerical modelling of spontaneous slab breakoff and subsequent topographic response. Tectonophysics, 502: 244–256

Duretz T, Schmalholz S M, Gerya T V. 2012. Dynamics of slab detachment. Geochem Geophys Geosyst, 13: Q03020

Duretz T, Agard P, Yamato P, Ducassou C, Burov E B, Gerya T V. 2016. Thermo-mechanical modeling of the obduction process based on the Oman ophiolite case. Gondwana Res, 32: 1–10

Eberle M A, Grasset O, Sotin C. 2002. A numerical study of the interaction between the mantle wedge, subducting slab, and overriding plate. Phys Earth Planet Inter, 134: 191–202

Ellis S M, Little T A, Wallace L M, Hacker B R, Buiter S J H. 2011. Feedback between rifting and diapirism can exhume ultrahigh-pressure rocks. Earth Planet Sci Lett, 311: 427–438

Erdman M E, Lee C T A. 2014. Oceanic- and continental-type metamorphic terranes: Occurrence and exhumation mechanisms. Earth-Sci Rev, 139: 33–46

Ernst W G. 2001. Subduction, ultrahigh-pressure metamorphism, and regurgitation of buoyant crustal slices—Implications for arcs and continental growth. Phys Earth Planet Inter, 127: 253–275

Ernst W G. 2005. Alpine and Pacific styles of Phanerozoic mountain building: Subduction-zone petrogenesis of continental crust. Terra Nova, 17: 165–188

Ernst W G, Maruyama S, Wallis S. 1997. Buoyancy-driven, rapid exhumation of ultrahigh-pressure metamorphosed continental crust. Proc Natl Acad Sci USA, 94: 9532–9537

Faccenda M, Gerya T V, Chakraborty S. 2008. Styles of post-subduction collisional orogeny: Influence of convergence velocity, crustal rheology and radiogenic heat production. Lithos, 103: 257–287

Faccenda M, Minelli G, Gerya T V. 2009. Coupled and decoupled regimes of continental collision: Numerical modeling. Earth Planet Sci Lett, 278: 337–349

Faure M, Lin W, Shu L, Sun Y, Scharer U. 1999. Tectonics of the Dabieshan (eastern China) and possible exhumation mechanism of ultra high-pressure rocks. Terra Nova, 11: 251–258

Fernández-García C, Guillaume B, Brun J P. 2019. 3D slab breakoff in laboratory experiments. Tectonophysics, 773: 228223

Ferrero S, Wunder B, Walczak K, O'Brien P J, Ziemann M A. 2015. Preserved near ultrahigh-pressure melt from continental crust subducted to mantle depths. Geology, 43: 447–450

Fossen H, Cavalcante G C, de Almeida R P. 2017. Hot versus cold orogenic behavior: Comparing the Araçuaí-West Congo and the Caledonian orogens. Tectonics, 36: 2159–2178

Funiciello F, Faccenna C, Giardini D. 2004. Role of lateral mantle flow in the evolution of subduction systems: Insights from laboratory experiments. Geophys J Int, 157: 1393–1406

Funiciello F, Faccenna C, Giardini D, Regenauer-Lieb K. 2003. Dynamics of retreating slabs: 2. Insights from three-dimensional laboratory experiments. J Geophys Res, 108: 2207

Garzanti E, Radeff G, Malusà M G. 2018. Slab breakoff: A critical appraisal of a geological theory as applied in space and time. Earth-Sci Rev, 177: 303–319

Gerya T V, Perchuk L L, Burg J P. 2008. Transient hot channels: Perpetrating and regurgitating ultrahigh-pressure, high-temperature crust-mantle associations in collision belts. Lithos, 103: 236–256

Gerya T V, Stöckhert B, Perchuk A L. 2002. Exhumation of high-pressure metamorphic rocks in a subduction channel: A numerical simulation. Tectonics, 21: 1056

Gerya T V, Yuen D A, Maresch W V. 2004. Thermomechanical modelling of slab detachment. Earth Planet Sci Lett, 226: 101–116

Goes S, Agrusta R, van Hunen J, Garel F. 2017. Subduction-transition zone interaction: A review. Geosphere, 13: 644–664

Göğüş O H, Pysklywec R N. 2008. Mantle lithosphere delamination driving plateau uplift and synconvergent extension in eastern Anatolia. Geology, 36: 723–726

Gonzalez-Castillo L, Galindo-Zaldivar J, de Lacy M C, Borque M J, Martinez-Moreno F J, García-Armenteros J A, Gil A J. 2015. Active rollback in the Gibraltar Arc: Evidences from CGPS data in the western Betic Cordillera. Tectonophysics, 663: 310–321

Gordon S M, Little T A, Hacker B R, Bowring S A, Korchinski M, Baldwin S L, Kylander-Clark A R C. 2012. Multi-stage exhumation of young UHP-HP rocks: Timescales of melt crystallization in the D'Entrecasteaux Islands, southeastern Papua New Guinea. Earth Planet Sci Lett, 351-352: 237–246

Gray R, Pysklywec R N. 2012. Geodynamic models of mature continental collision: Evolution of an orogen from lithospheric subduction to continental retreat/delamination. J Geophys Res, 117: 5733–5735

Guillot S, Hattori K H, Agard P, Schwartz S, Vidal O. 2009. Exhumation processes in oceanic and continental subduction contexts: A review. In: Lallemand S, Funiciello F, eds. Subduction Zone Geodynamics. Berlin Heidelberg: Springer. 175–205

Guillot S, Hattori K H, de Sigoyer J, Nägler T, Auzende A L. 2001. Evidence of hydration of the mantle wedge and its role in the exhumation of eclogites. Earth Planet Sci Lett, 193: 115–127

Hacker B R, Kelemen P B, Behn M D. 2011. Differentiation of the continental crust by relamination. Earth Planet Sci Lett, 307: 501–516

Hacker B R, Gerya T V. 2013. Paradigms, new and old, for ultrahigh-pressure tectonism. Tectonophysics, 603: 79–88

Hacker B R, Gerya T V, Gilotti J A. 2013. Formation and exhumation of ultrahigh-pressure terranes. Elements, 9: 289–293

Hacker B R, Ratschbacher L, Webb L, McWilliams M O, Ireland T, Calvert A, Dong S, Wenk H R, Chateigner D. 2000. Exhumation of ultrahigh-pressure continental crust in east central China: Late Triassic-Early Jurassic tectonic unroofing. J Geophys Res, 105: 13339–13364

Hall P S, Kincaid C. 2001. Diapiric flow at subduction zones: A recipe for rapid transport. Science, 292: 2472–2475

Hawkesworth C J, Cawood P A, Dhuime B. 2016. Tectonics and crustal evolution. GSA Today, 26: 4–11

Hermann J, Green D H. 2001. Experimental constraints on high pressure melting in subducted crust. Earth Planet Sci Lett, 188: 149–168

Hermann J, Müntener O, Scambelluri M. 2000. The importance of

serpentinite mylonites for subduction and exhumation of oceanic crust. Tectonophysics, 327: 225–238

Hermann J, Rubatto D. 2014. Subduction of continental crust to mantle depth: Geochemistry of ultrahigh-pressure rocks. In: Holland H D, Turekian K K, eds. Treatise on Geochemistry. 2nd ed. Oxford: Elsevier. 309–340

Hernández-Uribe D, Palin R M. 2019. A revised petrological model for subducted oceanic crust: Insights from phase equilibrium modelling. J Metamorph Geol, 37: 745–768

Herwartz D, Nagel T J, Münker C, Scherer E E, Froitzheim N. 2011. Tracing two orogenic cycles in one eclogite sample by Lu-Hf garnet chronometry. Nat Geosci, 4: 178–183

Herzberg C, Condie K C, Korenaga J. 2010. Thermal history of the Earth and its petrological expression. Earth Planet Sci Lett, 292: 79–88

Hodges K V. 2017. Subduction undone. Nature, 543: 44–45

Horton B K, Fuentes F. 2016. Sedimentary record of plate coupling and decoupling during growth of the Andes. Geology, 44: 647–650

Husson L, Brun J P, Yamato P, Faccenna C. 2009. Episodic slab rollback fosters exhumation of HP-UHP rocks. Geophys J Int, 179: 1292–1300

Hwang S L, Chu H T, Yui T F, Shen P, Schertl H P, Liou J G, Sobolev N V. 2006. Nanometer-size P/K-rich silica glass (former melt) inclusions in microdiamond from the gneisses of Kokchetav and Erzgebirge massifs: Diversified characteristics of the formation media of metamorphic microdiamond in UHP rocks due to host-rock buffering. Earth Planet Sci Lett, 243: 94–106

Ichikawa H, Kawai K, Yamamoto S, Kameyama M. 2015. Effect of water on subduction of continental materials to the deep earth. In: Khan A, Deschamps F, eds. The Earth's Heterogeneous Mantle: A Geophysical, Geodynamical, and Geochemical Perspective. Cham: Springer International Publishing. 275–299

Jiao R H, Herman F, Seward D. 2017. Late Cenozoic exhumation model of New Zealand: Impacts from tectonics and climate. Earth-Sci Rev, 166: 286–298

Kessel R, Schmidt M W, Ulmer P, Pettke T. 2005. Trace element signature of subduction-zone fluids, melts and supercritical liquids at 120–180 km depth. Nature, 437: 724–727

Kylander-Clark A R C, Hacker B R, Mattinson C G. 2012. Size and exhumation rate of ultrahigh-pressure terranes linked to orogenic stage. Earth Planet Sci Lett, 321-322: 115–120

Labrousse L, Duretz T, Gerya T. 2015. H_2O-fluid-saturated melting of subducted continental crust facilitates exhumation of ultrahigh-pressure rocks in continental subduction zones. Earth Planet Sci Lett, 428: 151–161

Labrousse L, Prouteau G, Ganzhorn A C. 2011. Continental exhumation triggered by partial melting at ultrahigh pressure. Geology, 39: 1171–1174

Lanari P, Engi M. 2017. Local bulk composition effects on metamorphic mineral assemblages. Rev Mineral Geochem, 83: 55–102

Langmuir C H, Klein E M, Plank T. 1992. Petrological systematics of mid-ocean ridge basalts: Constraints on melt generation beneath ocean ridges. Geophys Monogr, 71: 183–280

Leech M L. 2001. Arrested orogenic development: Eclogitization, delamination, and tectonic collapse. Earth Planet Sci Lett, 185: 149–159

Li B, Massonne H J. 2017. Contrasting metamorphic evolution of metapelites from the Malpica-Tuy unit and the underlying so-called parautochthon at the coast of NW Spain. Lithos, 286-287: 92–108

Li J L, Klemd R, Gao J, John T. 2016. Poly-cyclic metamorphic evolution of eclogite: Evidence for multistage burial-exhumation cycling in a subduction channel. J Petrol, 57: 119–146

Li L G, Liao X H, Fu R S. 2002. Slab breakoff depth: A slowdown subduction model. Geophys Res Lett, 29: 1041

Li S G, Jagoutz E, Chen Y Z, Li Q L. 2000. Sm-Nd and Rb-Sr isotopic chronology and cooling history of ultrahigh pressure metamorphic rocks and their country rocks at Shuanghe in the Dabie Mountains, Central China. Geochim Cosmochim Acta, 64: 1077–1093

Li Y, Yang Y, Liu Y C, Groppo C, Rolfo F. 2020a. Muscovite dehydration melting in silica-undersaturated systems: A case study from corundum-bearing anatectic rocks in the Dabie orogen. Minerals, 10: 213

Li Y, Liu Y C, Yang Y, Rolfo F, Groppo C. 2020b. Petrogenesis and tectonic significance of Neoproterozoic meta-basites and meta-granitoids within the central Dabie UHP zone, China: Geochronological and geochemical constraints. Gondwana Res, 78: 1–19

Li Z H, Xu Z Q, Gerya T V. 2011. Flat versus steep subduction: Contrasting modes for the formation and exhumation of high- to ultrahigh-pressure rocks in continental collision zones. Earth Planet Sci Lett, 301: 65–77

Liao J, Gerya T, Thielmann M, Webb A A G, Kufner S K, Yin A. 2017. 3D geodynamic models for the development of opposing continental subduction zones: The Hindu Kush-Pamir example. Earth Planet Sci Lett, 480: 133–146

Liao J, Malusà M G, Zhao L, Baldwin S L, Fitzgerald P G, Gerya T. 2018. Divergent plate motion drives rapid exhumation of (ultra)high pressure rocks. Earth Planet Sci Lett, 491: 67–80

Liou J G, Ernst W G, Zhang R Y, Tsujimori T, Jahn B M. 2009. Ultrahigh-pressure minerals and metamorphic terranes—The view from China. J Asian Earth Sci, 35: 199–231

Liou J G, Tsujimori T, Yang J, Zhang R Y, Ernst W G. 2014. Recycling

of crustal materials through study of ultrahigh-pressure minerals in collisional orogens, ophiolites, and mantle xenoliths: A review. J Asian Earth Sci, 96: 386–420

Little T A, Hacker B R, Gordon S M, Baldwin S L, Fitzgerald P G, Ellis S, Korchinski M. 2011. Diapiric exhumation of Earth's youngest (UHP) eclogites in the gneiss domes of the D'Entrecasteaux Islands, Papua New Guinea. Tectonophysics, 510: 39–68

Liu F L, Gerdes A, Liou J G, Xue H M, Liang F H. 2006. SHRIMP U-Pb zircon dating from Sulu-Dabie dolomitic marble, eastern China: Constraints on prograde, ultrahigh-pressure and retrograde metamorphic ages. J Metamorph Geol, 24: 569–589

Liu L P, Li Z X, Danišík M, Li S, Evans N, Jourdan F, Tao N. 2017. Thermochronology of the Sulu ultrahigh-pressure metamorphic terrane: Implications for continental collision and lithospheric thinning. Tectonophysics, 712-713: 10–29

Liu L, Zhang J, Green Ii H W, Jin Z, Bozhilov K N. 2007. Evidence of former stishovite in metamorphosed sediments, implying subduction to >350 km. Earth Planet Sci Lett, 263: 180–191

Liu L, Wang C, Cao Y T, Chen D L, Kang L, Yang W Q, Zhu X H. 2012. Geochronology of multi-stage metamorphic events: Constraints on episodic zircon growth from the UHP eclogite in the South Altyn, NW China. Lithos, 136-139: 10–26

Liu M Q, Li Z H, Yang S H. 2017. Diapir versus along-channel ascent of crustal material during plate convergence: Constrained by the thermal structure of subduction zones. J Asian Earth Sci, 145: 16–36

Liu P L, Wu Y, Liu Q, Zhang J F, Zhang L, Jin Z M. 2014. Partial melting of UHP calc-gneiss from the Dabie Mountains. Lithos, 192-195: 86–101

Liu Y C, Deng L P, Gu X F, Groppo C, Rolfo F. 2015. Application of Ti-in-zircon and Zr-in-rutile thermometers to constrain high-temperature metamorphism in eclogites from the Dabie orogen, central China. Gondwana Res, 27: 410–423

Liu Y C, Gu X F, Li S G, Hou Z H, Song B. 2011. Multistage metamorphic events in granulitized eclogites from the North Dabie complex zone, central China: Evidence from zircon U-Pb age, trace element and mineral inclusion. Lithos, 122: 107–121

Liu Y C, Li S G, Gu X F, Xu S T, Chen G B. 2007a. Ultrahigh-pressure eclogite transformed from mafic granulite in the Dabie orogen, east-central China. J Metamorph Geol, 25: 975–989

Liu Y C, Li S G, Xu S T. 2007b. Zircon SHRIMP U-Pb dating for gneisses in northern Dabie high *T*/*P* metamorphic zone, central China: Implications for decoupling within subducted continental crust. Lithos, 96: 170–185

Liu Y C, Liu L X, Li Y, Gu X F, Song B. 2017. Zircon U-Pb geochronology and petrogenesis of metabasites from the western Beihuaiyang zone in the Hong'an orogen, central China: Implications for detachment within subducting continental crust at shallow depths. J Asian Earth Sci, 145: 74–90

Lü Z, Bucher K, Zhang L F, Du J. 2012. The Habutengsu ultra-high pressure terrain of western Tianshan, China: Metamorphic evolution of metapelites and metagreywackes. J Metamorph Geol, 30: 907–926

Lü Z, Bucher K. 2018. The coherent ultrahigh-pressure terrane of the Tianshan meta-ophiolite belt, NW China. Lithos, 314-315: 260–273

Malusà M G, Faccenna C, Garzanti E, Polino R. 2011. Divergence in subduction zones and exhumation of high pressure rocks (Eocene Western Alps). Earth Planet Sci Lett, 310: 21–32

Malusà M G, Faccenna C, Baldwin S L, Fitzgerald P G, Rossetti F, Balestrieri M L, Danišík M, Ellero A, Ottria G, Piromallo C. 2015. Contrasting styles of (U)HP rock exhumation along the Cenozoic Adria-Europe plate boundary (Western Alps, Calabria, Corsica). Geochem Geophys Geosyst, 16: 1786–1824

Maruyama S, Liou J G, Zhang R Y. 1994. Tectonic evolution of the ultrahigh-pressure (UHP) and high-pressure (HP) metamorphic belts from central China. Island Arc, 3: 112–121

Massonne H J. 2001. First find of coesite in the ultrahigh-pressure metamorphic area of the central Erzgebirge, Germany. Eur J Mineral, 13: 565–570

Massonne H J. 2003. A comparison of the evolution of diamondiferous quartz-rich rocks from the Saxonian Erzgebirge and the Kokchetav Massif: Are so-called diamondiferous gneisses magmatic rocks? Earth Planet Sci Lett, 216: 347–364

Massonne H J. 2012. Formation of amphibole and clinozoisite-epidote in eclogite owing to fluid infiltration during exhumation in a subduction channel. J Petrol, 53: 1969–1998

Massonne H J. 2013. Constructing the pressure-temperature path of ultrahigh-pressure rocks. Elements, 9: 267–272

Menant A, Jolivet L, Tuduri J, Loiselet C, Bertrand G, Guillou-Frottier L. 2018. 3D subduction dynamics: A first-order parameter of the transition from copper- to gold-rich deposits in the eastern Mediterranean region. Ore Geol Rev, 94: 118–135

McKenzie D P. 1969. Speculations on the consequences and causes of plate motions. Geophys J Int, 18: 1–32

Meissner R, Mooney W. 1998. Weakness of the lower continental crust: A condition for delamination, uplift, and escape. Tectonophysics, 296: 47–60

Meyer M, Klemd R, John T, Gao J, Menneken M. 2016. An (in-) coherent metamorphic evolution of high-*P* eclogites and their host rocks in the Chinese southwest Tianshan? J Metamorph Geol, 34: 121–146

Moyen J F, van Hunen J. 2012. Short-term episodicity of Archaean plate tectonics. Geology, 40: 451–454

Nábělek J, Hetenyi G, Vergne J, Sapkota S, Kafle B, Jiang M, Su H, Chen J, Huang B S, Team H C. 2009. Underplating in the Himalaya-Tibet collision zone revealed by the Hi-CLIMB experiment. Science, 325: 1371–1374

Neubauer F, Lips A, Kouzmanov K, Lexa J, Ivaˇşcanu P. 2005. 1: Subduction, slab detachment and mineralization: The Neogene in the Apuseni Mountains and Carpathians. Ore Geol Rev, 27: 13–44

Niu Y L, Zhao Z D, Zhu D C, Mo X X. 2013. Continental collision zones are primary sites for net continental crust growth—A testable hypothesis. Earth-Sci Rev, 127: 96–110

O'Brien P J. 2019. Eclogites and other high-pressure rocks in the Himalaya: A review. Geol Soc Lond Spec Publ, 483: 183–213

Parrish R R, Gough S J, Searle M P, Waters D J. 2006. Plate velocity exhumation of ultrahigh-pressure eclogites in the Pakistan Himalaya. Geology, 34: 989–992

Peacock S M, Wang K. 1999. Seismic consequences of warm versus cool subduction metamorphism: Examples from southwest and northeast Japan. Science, 286: 937–939

Penniston-Dorland S C, Kohn M J, Manning C E. 2015. The global range of subduction zone thermal structures from exhumed blueschists and eclogites: Rocks are hotter than models. Earth Planet Sci Lett, 428: 243–254

Petersen K D, Buck W R. 2015. Eduction, extension, and exhumation of ultrahigh-pressure rocks in metamorphic core complexes due to subduction initiation. Geochem Geophys Geosyst, 16: 2564–2581

Palmer M R, Ersoy E Y, Akal C, Uysal İ, Genç Ş C, Banks L A, Cooper M J, Milton J A, Zhao K D. 2019. A short, sharp pulse of potassium-rich volcanism during continental collision and subduction. Geology, 47: 1079–1082

Platt J P. 1986. Dynamics of orogenic wedges and the uplift of high-pressure metamorphic rocks. Geol Soc Am Bull, 97: 1037–1053

Platt J P. 1993. Exhumation of high-pressure rocks: A review of concepts and processes. Terra Nova, 5: 119–133

Pusok A E, Kaus B J P, Popov A A. 2018. The effect of rheological approximations in 3-D numerical simulations of subduction and collision. Tectonophysics, 746: 296–311

Proyer A. 2003. The preservation of high-pressure rocks during exhumation: Metagranites and metapelites. Lithos, 70: 183–194

Ratschbacher L, Hacker B R, Webb L E, McWilliams M, Ireland T, Dong S, Calvert A, Chateigner D, Wenk H R. 2000. Exhumation of the ultrahigh-pressure continental crust in east central China: Cretaceous and Cenozoic unroofing and the Tan-Lu fault. J Geophys Res, 105: 13303–13338

Reinecke T. 1998. Prograde high- to ultrahigh-pressure metamorphism and exhumation of oceanic sediments at Lago di Cignana, Zermatt-Saas Zone, western Alps. Lithos, 42: 147–189

Ren Y F, Chen D L, Zhu X, Ren Z L, Gong X K, Luo F H. 2019. Two orogenic cycles recorded by eclogites in the Yuka-Luofengpo terrane: Implications for the Mesoproterozoic to early Paleozoic tectonic evolution of the North Qaidam orogenic belt, NW China. Precambrian Res, 333: 105449

Rosenbaum G, Gasparon M, Lucente F P, Peccerillo A, Miller M S. 2008. Kinematics of slab tear faults during subduction segmentation and implications for Italian magmatism. Tectonics, 27: TC2008

Rosenberg C L. 2001. Deformation of partially molten granite: A review and comparison of experimental and natural case studies. Int J Earth Sci, 90: 60–76

Rosenberg C L, Handy M R. 2005. Experimental deformation of partially melted granite revisited: Implications for the continental crust. J Metamorph Geol, 23: 19–28

Rubatto D, Hermann J. 2001. Exhumation as fast as subduction? Geology, 29: 3–6

Rubatto D, Regis D, Hermann J, Boston K, Engi M, Beltrando M, McAlpine S R B. 2011. Yo-yo subduction recorded by accessory minerals in the Italian Western Alps. Nat Geosci, 4: 338–342

Schellart W P. 2004. Kinematics of subduction and subduction-induced flow in the upper mantle. J Geophys Res, 109: B07401

Schellart W P, Stegman D R, Freeman J. 2008. Global trench migration velocities and slab migration induced upper mantle volume fluxes: Constraints to find an Earth reference frame based on minimizing viscous dissipation. Earth-Sci Rev, 88: 118–144

Schertl H P, Sobolev N V. 2013. The Kokchetav Massif, Kazakhstan: "Type locality" of diamond-bearing UHP metamorphic rocks. J Asian Earth Sci, 63: 5–38

Schliffke N, van Hunen J, Magni V, Allen M B. 2019. The role of crustal buoyancy in the generation and emplacement of magmatism during continental collision. Geochem Geophys Geosyst, 20: 4693–4709

Shreve R L, Cloos M. 1986. Dynamics of sediment subduction, melange formation, and prism accretion. J Geophys Res, 91: 10229–10245

Sizova E, Gerya T, Brown M. 2014. Contrasting styles of Phanerozoic and Precambrian continental collision. Gondwana Res, 25: 522–545

Sizova E, Gerya T, Brown M, Perchuk L L. 2010. Subduction styles in the Precambrian: Insight from numerical experiments. Lithos, 116: 209–229

Smith D C. 1984. Coesite in clinopyroxene in the Caledonides and its implications for geodynamics. Nature, 310: 641–644

Sobolev S V, Brown M. 2019. Surface erosion events controlled the evolution of plate tectonics on Earth. Nature, 570: 52–57

Sobolev N V, Shatsky V S. 1990. Diamond inclusions in garnets from

metamorphic rocks: A new environment for diamond formation. Nature, 343: 742–746

Solarino S, Malusà M G, Eva E, Guillot S, Paul A, Schwartz S, Zhao L, Aubert C, Dumont T, Pondrelli S, Salimbeni S, Wang Q C, Xu X B, Zheng T Y, Salimbeni S. 2018. Mantle wedge exhumation beneath the Dora-Maira (U)HP dome unravelled by local earthquake tomography (Western Alps). Lithos, 296-299: 623–636

Song S G, Niu Y L, Su L, Wei C J, Zhang L F. 2014a. Adakitic (tonalitic-trondhjemitic) magmas resulting from eclogite decompression and dehydration melting during exhumation in response to continental collision. Geochim Cosmochim Acta, 130: 42–62

Song S G, Niu Y L, Su L, Zhang C, Zhang L F. 2014b. Continental orogenesis from ocean subduction, continent collision/subduction, to orogen collapse, and orogen recycling: The example of the North Qaidam UHPM belt, NW China. Earth-Sci Rev, 129: 59–84

Su B, Chen Y, Mao Q. 2019. Sodium in olivine as a potential pressure indicator for orogenic dunite. Sci Bull, 65: 94–96

Stegman D R, Freeman J, Schellart W P, Moresi L, May D. 2006. Influence of trench width on subduction hinge retreat rates in 3-D models of slab rollback. Geochem Geophys Geosyst, 7: Q03012

Tamblyn R, Zack T, Schmitt A K, Hand M, Kelsey D, Morrissey L, Pabst S, Savov I P. 2019. Blueschist from the Mariana forearc records long-lived residence of material in the subduction channel. Earth Planet Sci Lett, 519: 171–181

Tang J, Zheng Y F, Wu Y B, Gong B. 2006. Zircon SHRIMP U-Pb dating, C and O isotopes for impure marbles from the Jiaobei terrane in the Sulu orogen: Implication for tectonic affinity. Precambrian Res, 144: 1–18

van Hunen J, Allen M B. 2011. Continental collision and slab break-off: A comparison of 3-D numerical models with observations. Earth Planet Sci Lett, 302: 27–37

van Keken P E, Hacker B R, Syracuse E M, Abers G A. 2011. Subduction factory: 4. Depth-dependent flux of H_2O from subducting slabs worldwide. J Geophys Res, 116: B01401

van Keken P E, Wada I, Abers G A, Hacker B R, Wang K. 2018. Mafic high-pressure rocks are preferentially exhumed from warm subduction settings. Geochem Geophys Geosyst, 19: 2934–2961

Wada I, Wang K. 2009. Common depth of slab-mantle decoupling: Reconciling diversity and uniformity of subduction zones. Geochem Geophys Geosyst, 10: Q10009

Wang H L, Huismans R S, Rondenay S. 2019. Water migration in the subduction mantle wedge: A two-phase flow approach. J Geophys Res-Solid Earth, 124: 9208–9225

Wang L, Kusky T M, Polat A, Wang S J, Jiang X F, Zong K Q, Wang J P, Deng H, Fu J M. 2014. Partial melting of deeply subducted eclogite from the Sulu orogen in China. Nat Commun, 5: 5604

Wang Q C, Cong B L. 1999. Exhumation of UHP Terranes: A case study from the Dabie Mountains, eastern China. Int Geol Rev, 41: 994–1004

Wang Y, Zhang L F, Li Z H, Li Q Y, Bader T. 2019. The exhumation of subducted oceanic-derived eclogites: Insights from phase equilibrium and thermomechanical modeling. Tectonics, 38: 1764–1797

Warren C J. 2013. Exhumation of (ultra-)high-pressure terranes: Concepts and mechanisms. Solid Earth, 4: 75–92

Warren C J, Beaumont C, Jamieson R A. 2008a. Formation and exhumation of ultra-high-pressure rocks during continental collision: Role of detachment in the subduction channel. Geochem Geophys Geosyst, 9: Q04019

Warren C J, Beaumont C, Jamieson R A. 2008b. Modelling tectonic styles and ultra-high pressure (UHP) rock exhumation during the transition from oceanic subduction to continental collision. Earth Planet Sci Lett, 267: 129–145

Webb L E, Baldwin S L, Little T A, Fitzgerald P G. 2008. Can microplate rotation drive subduction inversion. Geology, 36: 823–826

Weller O M, Copley A, Miller W G R, Palin R M, Dyck B. 2019. The relationship between mantle potential temperature and oceanic lithosphere buoyancy. Earth Planet Sci Lett, 518: 86–99

Whipple K X. 2014. Can erosion drive tectonics? Science, 346: 918–919

White R S, McKenzie D, O'Nions R K. 1992. Oceanic crustal thickness from seismic measurements and rare earth element inversions. J Geophys Res, 97: 19683–19,715

Wortel M J R, Spakman W. 2000. Subduction and slab detachment in the Mediterranean-Carpathian Region. Science, 290: 1910–1917

Wu Y, Fei Y W, Jin Z M, Liu X Y. 2009. The fate of subducted upper continental crust: An experimental study. Earth Planet Sci Lett, 282: 275–284

Xiao L, Wang C Z, Pirajno F. 2007. Is the underthrust indian lithosphere split beneath the Tibetan Plateau? Int Geol Rev, 49: 90–98

Xu J G, Zhang D Z, Fan D W, Dera P K, Shi F, Zhou W G. 2019. Thermoelastic properties of eclogitic garnets and omphacites: Implications for deep subduction of oceanic crust and density anomalies in the upper mantle. Geophys Res Lett, 46: 179–188

Xu S T, Okay A I, Ji S C, Sengor A M C, Su W, Liu Y C, Jiang L L. 1992. Diamond from the Dabie Shan Metamorphic Rocks and its implication for tectonic setting. Science, 256: 80–82

Xu S T, Liu Y C, Chen G B, Compagnoni R, Rolfo F, He M C, Liu H F. 2003. New finding of micro-diamonds in eclogites from Dabie-Sulu region in central-eastern China. Chin Sci Bull, 48: 988–994

Xu S T, Liu Y C, Su W, Wang R C, Jiang L L, Wu W P. 2000.

Discovery of the eclogite and its petrography in the Northern Dabie Mountain. Chin Sci Bull, 45: 273–278

Xu S T, Wu W P, Lu Y Q, Wang D H. 2012. Tectonic setting of the low-grade metamorphic rocks of the Dabie Orogen, central eastern China. J Struct Geol, 37: 134–149

Xu Z Q, Zeng L S, Liu F L, Yang J S, Zhang Z M, McWilliams M, Liou J G. 2006. Polyphase subduction and exhumation of the Sulu high-pressure-ultrahigh-pressure metamorphic terrane. Geol Soc Amer Spec Pap, 403: 93–113

Yamato P, Burov E, Agard P, Le Pourhiet L, Jolivet L. 2008. HP-UHP exhumation during slow continental subduction: Self-consistent thermodynamically and thermomechanically coupled model with application to the Western Alps. Earth Planet Sci Lett, 271: 63–74

Yamato P, Brun J P. 2017. Metamorphic record of catastrophic pressure drops in subduction zones. Nat Geosci, 10: 46–50

Yan L L, Zhang K J. 2019. Is exhumation of UHP terranes limited to low latitudes? J Geodyn, 130: 41–56

Yang J H, Cawood P A, Du Y S. 2010. Detrital record of mountain building: Provenance of Jurassic foreland basin to the Dabie Mountains. Tectonics, 29: TC4011

Ye K, Cong B, Ye D. 2000. The possible subduction of continental material to depths greater than 200 km. Nature, 407: 734–736

Yin A, Manning C E, Lovera O, Menold C A, Chen X, Gehrels G E. 2007. Early paleozoic tectonic and thermomechanical evolution of ultrahigh-pressure (UHP) metamorphic rocks in the Northern Tibetan Plateau, Northwest China. Int Geol Rev, 49: 681–716

Yoshida M. 2017. Trench dynamics: Effects of dynamically migrating trench on subducting slab morphology and characteristics of subduction zones systems. Phys Earth Planet Inter, 268: 35–53

Zhang H J, Wang F, Myhill R, Guo H. 2019. Slab morphology and deformation beneath Izu-Bonin. Nat Commun, 10: 1310

Zhang L F, Wang Y, Zhang L J, Lü Z. 2018. Ultrahigh pressure metamorphism and tectonic evolution of southwestern Tianshan orogenic belt, China: A comprehensive review. Geol Soc Lond Spec Publ, 474: 133–152

Zhang L F, Du J X, Lü Z, Yang X, Gou L L, Xia B, Chen Z Y, Wei C J, Song S G. 2013. A huge oceanic-type UHP metamorphic belt in southwestern Tianshan, China: Peak metamorphic age and *P-T* path. Chin Sci Bull, 58: 4378–4383

Zhao Z F, Zheng Y F, Chen Y X, Sun G C. 2017. Partial melting of subducted continental crust: Geochemical evidence from synexhumation granite in the Sulu orogen. Geol Soc Am Bull, 129: 1692–1707

Zheng Y F. 2012. Metamorphic chemical geodynamics in continental subduction zones. Chem Geol, 328: 5–48

Zheng Y F. 2019. Subduction zone geochemistry. Geosci Front, 10: 1223–1254

Zheng Y F, Zhou J B, Wu Y B, Xie Z. 2005. Low-grade metamorphic rocks in the Dabie-Sulu orogenic belt: A passive-margin accretionary wedge deformed during continent subduction. Int Geol Rev, 47: 851–871

Zheng Y F, Chen Y X. 2016. Continental versus oceanic subduction zones. Natl Sci Rev, 3: 495–519

Zheng Y F, Xia Q X, Chen R X, Gao X Y. 2011. Partial melting, fluid supercriticality and element mobility in ultrahigh-pressure metamorphic rocks during continental collision. Earth-Sci Rev, 107: 342–374

Zheng Y F, Zhao G. 2020. Two styles of plate tectonics in Earth's history. Sci Bull, 65: 329–334

Zheng Y F, Zhao Z F, Chen R X. 2019. Ultrahigh-pressure metamorphic rocks in the Dabie-Sulu orogenic belt: Compositional inheritance and metamorphic modification. Geol Soc Lond Spec Publ, 474: 89–132

(责任编委: 郑永飞)